치의과학박사 학위논문

Study on Accuracy of Orthognathic Surgery Using Virtual Surgical Planning

가상수술계획을 이용한 턱교정 수술의 정확도에 대한 연구

2021년 8월

서울대학교 대학원

치의과학과 구강악안면외과학전공

오 현 준

Study on Accuracy of Orthognathic Surgery Using Virtual Surgical Planning

가상수술계획을 이용한 턱교정 수술의 정확도에 대한 연구

지도 교수 서 병 무

이 논문을 치의과학박사 학위논문으로 제출함
2021년 5월

서울대학교 대학원
치의과학과 구강악안면외과학전공
오 현 준

오현준의 치의과학박사 학위논문을 인준함
2021년 7월

위 원 장 _____

부위원장 _____

위 원 _____

위 원 _____

위 원 _____

Abstract

Study on Accuracy of Orthognathic Surgery Using Virtual Surgical Planning

Hyun Jun OH, BS, MS, DDS

Oral and Maxillofacial Surgery Major, Department of Dentistry,

Graduate School, Seoul National University

(Directed by Professor **Byoung-Moo SEO**, DDS, MSD, PhD)

Purpose: In orthognathic surgery with three-dimensional virtual surgical planning, surgical accuracy has been investigated. However, there is no standardized method for assessing surgical accuracy, and detailed analysis of accuracy according to anatomic locations including the mandibular condyle, remains insufficient. The purpose of this study was to validate a computational method for one-time landmark setting and to analyze the degree and distribution of errors between the virtual plans and surgical outcomes according to anatomic locations.

Patients and Methods: This study included skeletal class III patients treated with both maxillary and mandibular surgeries by one operator. Virtual surgical planning in this study was based on cone beam computerized tomography (CBCT) and dental

model scan. Maxillofacial rapid prototyping (RP) models and surgical splints were fabricated using three-dimensional (3D) printing. Surgical guides for jaw osteotomy and pre-bent plates for fixation were fabricated on the RP models. Post-operative CBCT scans were obtained to evaluate surgical outcomes. Four anatomic locations consisting of the mandibular right and left condyles, maxilla, and distal segment of the mandible were analyzed using 10 landmarks. Landmarks were identified using the computational method based on affine transformation with one-time landmark setting. Agreement among measurements using the computational method was evaluated. Surgical accuracy was defined as the difference between the virtual plans and surgical outcomes. The accuracy was assessed using three kinds of errors: 1) a mean 3D distance error in the 3D Euclidean space, 2) mean absolute errors along the horizontal, vertical, and anteroposterior axes, and 3) mean signed errors along the three axes. The mean signed errors were visualized with multi-dimensional scattergrams. Bivariate and regression statistics were computed to measure the association between the anatomic location and surgical accuracy. Surgical accuracy according to the surgical plan for the maxilla and the accuracy according to the error in the maxilla were analyzed to investigate the factors affecting the accuracy.

Results: This study included 52 patients, 26 men and 26 women, with a mean age of 21 years and 3 months. The computational method for one-time landmark setting demonstrated excellent agreement among the measurements. The mean 3D distance errors for the mandibular right and left condylar landmarks, maxillary landmarks, and landmarks on the distal segment of the mandible were 0.95, 1.12, 1.25, and 2.24 mm, respectively. The largest mean absolute errors among the three axes for the

mandibular right and left condylar landmarks and the landmarks on the distal segment of the mandible were 0.51, 0.66, and 1.40 mm along the vertical axis, respectively. The largest mean absolute errors among the three axes for maxillary landmarks was 0.68 mm along the anteroposterior axis. The mean signed errors showed that the mandibular right and left condylar landmarks and the landmarks on the distal segment of the mandible were positioned 0.42, 0.57, and 1.25 mm inferior, respectively, and the maxillary landmarks were positioned 0.28 mm anterior to the planned position. The landmark errors for the distal segment of the mandible exhibited wider distributions compared to those for the condylar and maxillary landmarks. The errors for the condyles and maxilla were higher in maxillary setback than in maxillary advancement. The errors for the distal segment of the mandible were higher in cases where the amount of the maxillary impaction was smaller than the amount planned.

Conclusion: The landmark setting method in this study can be applied reliably for assessment of surgical accuracy in orthognathic surgery. Among the anatomic locations, the mandibular right and left condyles were the most accurate in orthognathic surgery using virtual surgical planning, followed by the maxilla, and the distal segment of the mandible. The accuracy was affected by the surgical plan for the maxilla and the error in the maxilla. For accurate orthognathic surgery, it is important to consider the tendency for surgical errors in each anatomic location.

Keywords: Surgical accuracy; Orthognathic surgery; Virtual surgical planning; Skeletal class III malocclusion; Affine transformation

Student Number: 2017-32052

Contents

---

* This PhD dissertation includes the contents of Hyun Jun OH *et al.*'s published paper, "Virtually-Planned Orthognathic Surgery Achieves an Accurate Condylar Position. Journal of Oral and Maxillofacial Surgery. 2021 May;79(5):1146.e1-1146.e25."

I. Introduction

Orthognathic surgery, also known as corrective jaw surgery, is designed to correct maxillary and mandibular conditions related to malocclusion issues due to skeletal disharmonies or congenital deformities [1]. When growth of the maxilla or mandible deviates from normal growth and exhibits excess, deficiency, or asymmetry, orthognathic surgery corrects variations in shape and size [2].

The accuracy of surgical planning and planned surgery is essential for the success of orthognathic surgery [3]. Traditional treatment planning for orthognathic surgery depends on two-dimensional (2D) cephalometric analysis and the study of plaster dental models. The conventional process has some drawbacks that include being a labor-intensive procedure that is time-consuming and potentially inaccurate due to head positioning errors [4-6]. The conventional method has inherent limitations due to the 2D analysis as a projection of the three-dimensional craniofacial complex. Moreover, due to the different planning steps for cephalometric tracing, face-bow transfer, model surgery, and surgical splint fabrication, errors are transferred to each of the subsequent steps and accumulate [7, 8]. Virtual surgical planning produces more accurate surgical outcomes than the conventional method by removing errors related to the laboratory processes [9].

Virtual planning with three-dimensional cephalometric analysis and surgical procedures were integrated with the transfer of planning into the surgical field using surgical splints [10-12]. Three-dimensional (3D) printed rapid prototyping (RP) models, 3D printed surgical splints, and customized surgical guides have greatly improved surgical planning which has resulted in more favorable surgical outcomes

[13-16]. However, previous studies lack consensus concerning accuracy assessment [17], and studies that assessed the accuracy of mandibular condyle areas between virtual plans and surgical outcomes in orthognathic surgery using 3D virtual planning systems have been insufficient.

To evaluate surgical accuracy, superimposition of the virtual plan and surgical outcome is needed. Three kinds of registration methods for superimposition have been introduced in the literature [18]: landmark based registration [19, 20], surface based registration [21], and voxel based registration [22, 23]. Surface and voxel based registrations are not significantly different, while landmark based registration is reliable but less accurate than the other methods according to recent studies [24, 25]. The clinical acceptance of surgical accuracy was considered in previous publications, and the criterion suggested was a linear difference less than 2 mm between the virtual plan and surgical outcome [26-30].

The purpose of this study was to validate a computational method for superimposition that was based on a mathematical analysis with the affine transformation of a rigid body and to analyze quantitatively the accuracy of orthognathic surgery by applying 3D virtual surgical planning using the computational method. It was hypothesized that differences between the virtual plan and surgical outcome after applying the 3D virtual surgical planning system could be negligible regardless of any landmarks used in this study. The specific aims of this study were to identify the deviation of landmarks for each segment in three different planes, which were visualized as multi-dimensional scattergrams.

II. Patients and Methods

1. Study design and subjects

A retrospective cohort study was designed. The study population was composed of all consecutive patients with skeletal class III malocclusion operated at the Department of Oral and Maxillofacial Surgery, Seoul National University Dental Hospital between July 1, 2014 and February 28, 2018. Inclusion criteria were orthognathic surgery on both the maxilla and mandible with or without genioplasty. Exclusion criteria were a single jaw operation, jaw segmentation, and congenital deformities such as cleft lip/palate or other craniofacial synostoses. The orthognathic surgeries were Le Fort I osteotomies for maxilla and bilateral sagittal split ramus osteotomies (BSSRO) for mandible. All the operations were performed by one surgeon (B. M. SEO). Due to the retrospective nature of this study, obtaining patients' informed consent was waived, and the study was approved by the Institutional Review Board at Seoul National University Dental Hospital (IRB approval number ERI19011).

2. Anatomic locations and landmarks

During bimaxillary orthognathic surgery, maxilla and mandible are osteotomized into bone segments. It was postulated that surgical accuracy might be different according to anatomic locations where the osteotomized bone segments were located. Therefore, the anatomic locations were composed of four different segments: the right and left condyle on the proximal segment of the mandible, maxilla, and the distal segment of the mandible. Three-dimensional coordinates were evaluated for the 10 anatomic landmarks that comprised the central incisors, right and left first molars of the maxilla and mandible, Point A, Point B, and the left and right condyles (Table 1). The landmarks of the upper and lower central incisors were defined as U1 and L1, respectively. U1 was set as the midpoint between the midpoint of the incisal edge of the upper right central incisor and the midpoint of the incisal edge of the upper left central incisor. L1 was set as the midpoint between the midpoint of the incisal edge of the lower right central incisor and the midpoint of the incisal edge of the lower left central incisor. The mesiobuccal cusp tips were used as the landmarks for the first molars. The landmarks of the right condyle and left condyle were defined as the midpoint of the rectangles formed by the tangent lines around the condyle heads, as illustrated in Figure 1. Biologically relevant variables such as age and sex were included. Surgical accuracy was investigated using three kinds of errors: mean three-dimensional distance error calculated from the three-dimensional Euclidean distance, mean absolute error and mean signed error along the horizontal, vertical, and anteroposterior axes, between the virtual plan and surgical outcome.

3. Protocol of virtual surgical planning, operation, and analysis

The workflow of the protocol was based on the previous study [31] and is illustrated in Figure 2. The system applied in this study consisted of a 3D virtual surgical planning system based on cone beam computed tomography (CBCT) data and 3D scanned dental models. Centric Relation (CR) bite was obtained using a wax plate, and pre-operative CBCTs were taken with the wax bite approximately 2–3 weeks before the operation. The voxel size was 0.39 mm x 0.39 mm x 0.39 mm, and the field of view was 200 mm x 179 mm in the CBCT scanner (Alphard-3030; ASAHIROENTGEN, Kyoto, Japan). Dental plaster models were scanned with the same wax bite using an optical scanner (inEos X5; Sirona, Charlotte, NC, USA). Pre-operative 3D CBCT data was reoriented using the Frankfort horizontal plane with reference to 3D cephalometric landmarks such as the orbitales and nasion. The lateral orbital rim area and clinical photos were also referenced. The pre-operative CBCT data and the scanned models were superimposed using reverse engineering software (Rapidform XOR3; INUS Technology, Seoul, Korea). Three-dimensional imaging software (Invivo 5; Anatomage, San Jose, CA, USA) and 3D Computer aided design (CAD) software (Magics 18; Materialise, Leuven, Belgium) were used for virtual planning and analysis. Final occlusion was established with the plaster models, and the information on the final occlusion was transferred to the 3D CAD software through repetitive transformation. RP models, an intermediate splint, and a final splint were fabricated using 3D printing (ProJet460Plus; 3D Systems, Rock Hill, SC, USA). Surgical guides for the osteotomies, based on the amount of surgical movement, were fabricated on the RP models and used during the operation [31]. Mandibular plates (BOS plate; BioMaterials Korea, Seoul, Korea) were pre-bent on

the RP models.

In all cases, Le Fort I osteotomy for the maxilla was performed first and BSSRO for the mandible was followed. Two screws (Dual Top Anchor system; Jeil Medical, Seoul, Korea) were installed on the nasion and interdental area between the root apices of the right and left upper central incisors for vertical reference. The maxilla was osteotomized first using the surgical template and relocated to the planned position, then fixated with a plating system (Leibinger Universal 2; Stryker, Kalamazoo, MI, USA) while intermaxillary fixation was applied using an intermediate splint. Before the fixation of the maxilla was performed, the vertical distance between two screws was checked. Moreover, the amount of bony segment movement on the RP model was checked. The next step was mandibular osteotomy using the surgical template with prefabricated drilling holes. After completion of the mandibular osteotomy, the possible interference area was removed. Before the fixation of the mandible, the passive adaptation of the pre-bent plate was checked. The surgical splints also functioned as condyle positioning devices [31]. The wings of the intermediate and final splints were in contact with the anterior ramus of the mandible, and the vertical position of the proximal segments should be on the same level as these wings. Therefore, these can serve as condylar positioning devices. In the intermaxillary fixation state with the final splint, mandibular segments were secured with pre-bent plates. After the fixation of the mandible, in the intermaxillary fixation state, the maxillary fixation was temporarily released and any possible interference was checked. The posterior part of the maxilla was carefully checked, and if there was residual interference, the interference was removed. The maxilla was finally fixated again. The effect of mandible-first surgery was obtained using

this surgical protocol. This is because the operated mandible can be used as a comparable reference for a non-operated mandible if the operation was performed as planned to locate the positions of screw holes and plates. Afterwards, intermaxillary fixation was released, and passive occlusal guidance was assessed.

As the final splint was placed with tight boxing using elastics, a transcranial view was taken to check the condylar position on the morning of post-operative day one, and post-operative CBCTs were taken approximately 1–2 week(s) after the operation.

4. Computational method for one-time landmark setting

The mathematical processing was based on the transformation of a rigid body. At first, the landmarks were manually configured on the pre-operative 3D data using Invivo 5 software which supports a 0.01 mm level of precision. Afterward, the surgical outcomes were superimposed with the pre-operative 3D data using the cranial base, zygomatic bone, and frontal bone, all areas unaffected by the surgery [23, 32]. Voxel-based registration was used for the superimposition in this study and was performed repetitively for checking axial, coronal, and sagittal planes using Invivo 5. Subsequently, the maxilla, right proximal segment of the mandible, left proximal segment of the mandible, and distal segment of the mandible were superimposed. Areas unaffected by the surgery were also used as mutual reference. Areas included teeth, the incisive foramen, and hard palate for the superimposition of the maxilla. Areas including teeth, the mental foramen, and inferior alveolar nerve canal were used for the superimposition of the distal segment of the mandible. Areas that included the coronoid process and the shape and trabeculae pattern of the condyles were used to superimpose the proximal segments. Three-dimensional

transformation can be represented as an affine transformation of a rigid body [33, 34]. The transformation matrix that contained information for translation and rotation was calculated, and as a result, the amount of movement in 3D space was derived using the quaternion operation [31, 35]. The system in the present study required setting the anatomic landmarks only from the pre-operative 3D data.

Using this method, it was not necessary to repeat positioning of the landmarks. The landmarks in the virtual plan and surgical outcome could be calculated by a transformation matrix as follows:

$$Landmark_{plan} = V \cdot Landmark_{pre-OP}$$
$$Landmark_{outcome} = S \cdot Landmark_{pre-OP} \quad (1)$$

where $Landmark_{pre-OP}$ is the landmark in pre-operative 3D data, $Landmark_{plan}$ is the landmark in the virtual plan, $Landmark_{outcome}$ is the landmark in the surgical outcome, V is the transformation matrix by the virtual plan and S is the transformation matrix by surgery (Figure 3). Therefore, mathematical tracking of these anatomic landmarks was possible using affine transformation of a rigid body based on voxel based registration without repetitively identifying landmarks.

Mathematically, there are three principal methods to propagate the orientation information: Euler, direction cosine matrix (DCM), and quaternion (Figure 3). Transformations among the three methods can be utilized [36-38]. The information on the transformation by surgery was initially stored in a quaternion format. Thereafter, the quaternions were transformed into Euler representations for angular

operations. Afterward, X-coordinate, Y-coordinate, and Z-coordinate representations were obtained using the DCM method for more intuitive forms.

5. Error definition

The three axes consistent with the Cartesian coordinate system were configured. The X-axis represented the horizontal axis, the Y-axis represented the vertical axis, and Z-axis represented the anteroposterior axis. Positive values for the axes were configured as left, superior, and anterior directions. Errors between the virtual plans and surgical outcomes were defined as surgical accuracy and calculated in the 3D Cartesian coordinate system [39]. The surgical accuracy was defined in reverse relation with the errors. That is, the closer the error came to 0, the higher the level of surgical accuracy.

Three kinds of errors were investigated. The first errors were mean absolute errors that occurred along each axis and were calculated for each axis as follows:

$$\begin{aligned} &Mean\ \ absolute\ \ error \\ &= Mean\ \ \left|Landmark_{outcome} - Landmark_{plan}\right| \\ &= (Mean\left|x_{outcome} - x_{plan}\right|, Mean\left|y_{outcome} - y_{plan}\right|, Mean\left|z_{outcome} - z_{plan}\right|)^T \end{aligned} \quad (2)$$

where $Landmark_{outcome}$ is $(x_{outcome}, y_{outcome}, z_{outcome})^T$ and $Landmark_{plan}$ is $(x_{plan}, y_{plan}, z_{plan})^T$.

The second errors were mean errors that occurred along each axis as follows:

$$Mean\ \ signed\ \ error = Mean\ \ (Landmark_{outcome} - Landmark_{plan}) \quad (3)$$

The third error was mean 3D distance error calculated as the mean Euclidean distance, which was the magnitude of the mean absolute error vector or mean error vector as follows:

$$\begin{aligned} &Mean\ 3D\ distance\ error \\ &= Mean\ \left\|Landmark_{outcome} - Landmark_{plan}\right\| \\ &= \frac{1}{n}\sum_{i=1}^{n}\sqrt{(x_{outcome,i} - x_{plan,i})^2 + (y_{outcome,i} - y_{plan,i})^2 + (z_{outcome,i} - z_{plan,i})^2} \end{aligned} \quad (4)$$

The differences between the virtual plans and surgical outcomes were calculated using vector operations. The mean absolute errors were the mean magnitudes of the errors that occurred along each axis. The mean signed errors were the mean directions of the errors that occurred along each axis. The mean 3D distance error was the mean magnitude of the error that occurred in 3D space. Three kind of errors were illustrated in Figure 4.

6. Accuracy according to surgical plan for maxilla and error in maxilla

The accuracy of the maxilla, right and left condyles, and the distal segment of the mandible according to surgical plan for the maxilla were investigated. The maxillary anteroposterior plan consisted of maxillary advancement and maxillary setback. Since most of the surgical plans for the maxilla were vertical impaction (superior positioning), subjects who had plan of the maxillary impaction were assessed. The mean signed errors of each anatomic location were evaluated according to whether the anteroposterior plan for the maxilla was advancement or setback.

The accuracy of the anatomic locations except the maxilla according to error in the maxilla were analyzed. Vertical errors in the maxilla were divided into over-impaction and under-impaction. The over-impaction or under-impaction was defined as a case in which the amount of maxillary impaction was larger or smaller than planned, respectively. The mean signed errors were evaluated according to whether the vertical error in the maxilla was the over-impaction or under-impaction.

7. Statistical analysis

The statistical analyses were performed using Language R (Vienna, Austria) [40]. In order to verify the reliability of the superimposition method, one researcher performed this process twice on the data set from 10 randomly selected subjects at an interval of one week, while the other researcher independently performed the superimposition one more time. A total of three superimpositions were performed to assess reproducibility. The reproducibility was evaluated using reliability and agreement measures [41-43]. Intraclass correlation coefficients (ICC) were used as a reliability measure, and Bland and Altman plots were employed as an agreement measure in this study. Intra-observer and inter-observer reliability, according to the ICC, were calculated. The two-way mixed effects model with the single measurement (not the average measurements) type and the absolute agreement definition was used [44, 45]. Bland and Altman plots were drawn to evaluate the agreement with 95% limits of agreement [46].

Mean 3D distance errors, mean absolute errors, and mean signed errors were analyzed with one-sample *t*-tests to assess whether the errors were significantly different from 0. To control for multiplicity problems, *t*-tests with the Bonferroni correction for alpha errors were performed. Multi-dimensional scattergrams for the mean signed errors on the sagittal, coronal, and horizontal planes were drawn using Language R [40], and the tendency of the errors was visualized and analyzed in each plane [47]. The contour of an ellipse in the scattergram indicated a 95% confidence boundary [48, 49].

Bivariate statistics were computed to identify age, sex, and anatomic location associated with mean 3D distance errors. The anatomic location as primary predictor

and age and sex as biologically relevant variables were included in a multiple linear regression model to determine the adjusted associations. For all analyses, a *P* value less than .05 was considered statistically significant.

The results from the recent studies analyzing accuracy in orthognathic surgery using 3D virtual planning were compared with the results from this study. Student's *t*-tests and Student-Newman-Keuls multiple comparison tests were performed to compare this study's accuracy with recent studies using the SNK testers - Multiple comparison program (SNU Industry Foundation, Seoul, Korea). Using the same landmarks, errors for the maxillary right and left first molars in Ritto et al.'s study [30], and similar landmarks, errors for the maxillary right and left first molars, mandibular right and left first molars, and maxillary and mandibular central incisors in Zhang et al.'s study [29] were compared statistically.

III. Results

1. Detailed description of study subjects

The present study included 52 patients (26 men and 26 women) who had skeletal class III malocclusion (Table 2). The mean age of the patients was 21 years and 3 months old. The age range was from 16 years and 11 months old to 28 years and 1 month old. Fourteen patients among the 52 patients underwent genioplasty. Only two patients (19 years old female and 23 years 7 months old male) among 52 patients underwent re-fixation surgery on the post-operative day 4 and day 1, respectively, due to inappropriate condyle positioning and unstable occlusion. The mean period of post-operative orthodontic treatment for the 45 traceable patients among the 52 patients was 9 ± 5 months.

The vertical surgical plans for the maxilla in this study were composed of maxillary impaction for 48 patients, no vertical movement for one patient, and maxillary elongation (inferior positioning) for three patients. The anteroposterior and vertical plans for mandible were setback and impaction, respectively because the subjects in this study had skeletal class III malocclusion.

2. Validation for landmark setting method

To evaluate the reliability of the measurements, intra-observer intraclass correlation coefficients (ICC) and inter-observer ICC were calculated (Table 3). Each coordinate exhibited excellent intra-observer reliability ranging from 0.9962 to 1.0000 and excellent inter-observer reliability ranging from 0.9897 to 1.0000. To evaluate the agreement among the measurements, Bland and Altman plots were used. The Bland-Altman plots for all the landmarks showed an excellent agreement among the three measurements. The Bland and Altman plots for the right condyle are representatively illustrated. (Figure 5). Since there was no obvious trend in the plots, the measurement errors were independent of the coordinates for the post-operative outcomes. The mean differences between the measurements were close to 0, representing negligible bias. The upper and lower limits of agreements were small. The differences between the measurements were within the limits of agreements with few outliers.

3. Accuracy according to anatomic location

3.1 Mean 3D distance error

The mean 3D distance error for the right condylar landmark, the left condylar landmark, maxillary landmarks, and the landmarks on the distal segment of the mandible was 0.95 ± 0.68 mm, 1.12 ± 0.62 mm, 1.25 ± 0.60 mm, and 2.24 ± 1.15 mm, respectively (Table 4). There was a significant difference among the segments and the mean 3D distance errors for all the segments were significantly different from 0 mm (Table 4). The mean 3D distance error for each landmark is illustrated in Figure 6.

The anatomic locations were accurate in the following order by the mean 3D distance error: the mandibular condyles, maxilla, and distal segment of the mandible.

3.2 Mean absolute error

Mean absolute errors on the X-coordinate, Y-coordinate, and Z-coordinate of the right condylar landmark were 0.49 ± 0.43 mm, 0.51 ± 0.53 mm, and 0.45 ± 0.45 mm, respectively. The mean absolute errors on the X-coordinate, Y-coordinate, and Z-coordinate of the left condylar landmarks were 0.58 ± 0.52 mm, 0.66 ± 0.54 mm, and 0.44 ± 0.32 mm, respectively. The mean absolute errors on the X-coordinate, Y-coordinate, and Z-coordinate of the maxillary landmarks were 0.66 ± 0.49 mm, 0.57 ± 0.49 mm, and 0.68 ± 0.48 mm, respectively. The mean absolute errors on the X-coordinate, Y-coordinate, and Z-coordinate of the landmarks on the distal segment of mandible were 0.96 ± 0.76 mm, 1.40 ± 1.11 mm, and 1.0 ± 0.82 mm, respectively.

There was a significant difference among the segments and the mean absolute errors for all the segments were significantly different from 0 mm (Table 4).

The anatomic locations were accurate in the following order by the mean absolute error: the mandibular condyles, maxilla, and distal segment of the mandible on the X- and Z-coordinates. On the Y-coordinate, the mean absolute errors for the mandibular condyles were similar to those for the maxilla. The errors for the distal segment of mandible were higher than those for the other anatomic locations.

3.3 Mean signed error

Mean signed errors on the X-coordinate, Y-coordinate, and Z-coordinate of the right condylar landmark were -0.23 ± 0.61 mm (P = .4012), -0.42 ± 0.61 mm (P = .0004), and -0.09 ± 0.63 mm (P = 1.0000), respectively. Mean signed errors on the X-coordinate, Y-coordinate, and Z-coordinate of the left condylar landmark were 0.32 ± 0.71 mm (P = .0907), -0.57 ± 0.64 mm (P < .0001), and -0.17 ± 0.52 mm (P = 1.0000), respectively. The mean signed errors on the X-coordinate, Y-coordinate, and Z-coordinate of maxillary landmarks were -0.04 ± 0.82 mm (P = 1.0000), 0.07 ± 0.75 mm (P = 1.0000), and 0.28 ± 0.79 mm (P < .0001), respectively. The mean signed errors on the X-coordinate, Y-coordinate, and Z-coordinate of the landmarks on the distal segment of the mandible were 0.23 ± 1.20 mm (P = .2492), -1.25 ± 1.27 mm (P < .0001), and -0.11 ± 1.29 mm (P = 1.0000), respectively (Table 5). The mean signed errors for each landmark are presented in Table 5 and visualized in Figure 7.

The anatomic locations were accurate in the following order by the mean signed error: the mandibular condyles, maxilla, and distal segment of mandible. The

proximal and distal segments of the mandible were positioned inferior and the maxilla was positioned anterior to the planned position.

3.4 Multi-dimensional scattergram for mean signed error

The mean signed errors on the sagittal, coronal, and horizontal planes were visualized with multi-dimensional scattergrams. The errors of the landmarks for the right and left condyles are illustrated in Figure 8. The errors of the right and left condyles tended to be downward and slightly outward.

The mean signed errors at the maxillary and mandibular first molar landmarks are illustrated in Figure 9. The errors for the maxillary first molars were lower than the errors for the mandibular first molars in the XY, ZY, and XZ planes. The mean signed errors of the maxillary first molars tended to be slightly forward. The mean signed errors of the mandibular first molars tended to be downward.

The errors for the landmarks at U1, Point A, L1, and Point B are illustrated in Figure 10. The errors for U1 and Point A were smaller than the errors for L1 and Point B, respectively. The mean errors for U1 and Point A tended to be slightly forward. The mean errors for L1 tended to be downward and slightly left. The mean errors for Point B tended to be directed downward, backward, and slightly left.

The errors for the distal segment of the mandible exhibited wider distributions compared to those for the mandibular condyles and maxilla.

3.5 Multiple linear regression for mean 3D distance error

Bivariate analyses showed that there was no association between sex and mean 3D distance error in Table 6 ($P = .1660$). Moreover, age was not significantly associated with mean 3D distance error ($P = .0620$). There was a significant difference among the anatomic locations ($P < .0001$).

The results obtained from multiple linear regression analysis are presented in Table 7. For patient characteristics, the mean 3D distance errors were not significantly different according to age and sex. On the contrary, there was a significant difference in the mean 3D distance errors according to the anatomic location. The right condyle had the smallest error, and no significant difference between the left and right condyles was observed. The largest error was found in the distal segment of the mandible, which was about 1.29 mm greater than the right condyle. The mean 3D distance error for the maxilla was about 0.30 mm greater than the right condyle and about 0.99 mm smaller than the distal segment of the mandible. There was a significant difference between the maxilla and the right condyle. Moreover, there were significant differences between the distal segment of the mandible and all other segments.

The anatomic location significantly affected the surgical accuracy.

4. Accuracy according to surgical plan for maxilla

Among 52 subjects, surgical plans for the maxilla were vertical impaction in 48 subjects (Table 2). The surgical plan for the maxilla was defined as an average surgical plan of U1, Point A, #16, and #26. To analyze the direction of errors, 48 subjects planned for the maxillary impaction were investigated. The error patterns of Point A according to surgical plans for the maxilla are described in Table 8 and Figure 11. When the surgical plans for the maxilla were impaction and advancement, mean signed errors on the X-coordinate, Y-coordinate, and Z-coordinate of Point A were 0.00 ± 0.91 mm (P = 1.0000), -0.16 ± 0.74 mm (P = 1.0000), and 0.05 ± 0.70 mm (P = 1.0000), respectively. When the plans for the maxilla were impaction and setback, the mean signed errors on the X-coordinate, Y-coordinate, and Z-coordinate of Point A were -0.12 ± 0.78 mm (P = 1.0000), -0.46 ± 0.69 mm (P = .3470), and 0.57 ± 0.51 mm (P = .0047), respectively. In subjects with maxillary impaction, the errors in the maxilla for maxillary setback were significantly upward (P = .0054) and significantly forward (P = .0080) compared to those for maxillary advancement.

The error patterns of mandibular condyles according to surgical plans for the maxilla are described in Table 8 and Figure 11. When the plans for the maxilla were impaction and advancement, the mean signed errors on the X-coordinate, Y-coordinate, and Z-coordinate of the right condyle were -0.24 ± 0.46 mm (P = .3285), -0.17 ± 0.37 mm (P = .7362), and -0.21 ± 0.49 mm (P = 1.0000), respectively. When the plans for maxilla were impaction and setback, the mean signed errors on the X-coordinate, Y-coordinate, and Z-coordinate of the right condyle were -0.18 ± 0.77 mm (P = 1.0000), -0.76 ± 0.74 mm (P = .0105), and 0.13 ± 0.81 mm (P = 1.0000), respectively. When the surgical plans for the maxilla were impaction and

advancement, the mean signed errors on the X-coordinate, Y-coordinate, and Z-coordinate of the left condyle were 0.33 ± 0.76 mm (P = .9986), -0.44 ± 0.47 mm (P < .0001), and -0.19 ± 0.57 mm (P = 1.0000), respectively. When the plans for the maxilla were impaction and setback, the mean signed errors on the X-coordinate, Y-coordinate, and Z-coordinate of the left condyle were 0.31 ± 0.71 mm (P = 1.0000), -0.76 ± 0.67 mm (P = .0041), and -0.14 ± 0.50 mm (P = 1.0000), respectively. In subjects with maxillary impaction, the errors of the right condyle for maxillary setback were significantly downward compared to those for maxillary advancement (P = .0035).

The error patterns of Point B according to surgical plans for the maxilla are described in Table 8 and Figure 11. When the surgical plans for the maxilla were impaction and advancement, the mean signed errors on the X-coordinate, Y-coordinate, and Z-coordinate of Point B were 0.45 ± 1.37 mm (P = 1.0000), -1.72 ± 1.44 mm (P < .0001), and -1.10 ± 1.45 mm (P = .0123), respectively. When the plans for the maxilla were impaction and setback, the mean signed errors on the X-coordinate, Y-coordinate, and Z-coordinate of Point B were 0.16 ± 0.95 mm (P = 1.0000), -1.06 ± 1.09 mm (P = .0182), and 0.06 ± 1.34 mm (P = 1.0000), respectively. In subjects with maxillary impaction, the errors in the mandible for maxillary advancement were significantly backward compared to those for maxillary setback (P = .0075).

The anteroposterior plan for the maxilla was thought to be one of the factors affecting the surgical accuracy in four anatomic locations.

5. Accuracy according to error in maxilla

The error patterns in mandibular condyles according to errors in the maxilla are described in Table 9 and Figure 12. The error in the maxilla was defined as an average error of U1, Point A, #16, and #26. When the vertical errors in the maxilla involved over-impaction, the mean signed errors on the X-coordinate, Y-coordinate, and Z-coordinate of the right condyle were -0.30 ± 0.61 mm (P = .4992), -0.55 ± 0.63 mm (P = .0033), and -0.03 ± 0.60 mm (P = 1.0000), respectively. When the vertical errors in the maxilla involved under-impaction, the mean signed errors on the X-coordinate, Y-coordinate, and Z-coordinate of the right condyle were -0.11 ± 0.57 mm (P = 1.0000), -0.21 ± 0.54 mm (P = 1.0000), and -0.12 ± 0.72 mm (P = 1.0000), respectively. When the vertical errors in the maxilla involved over-impaction, the mean signed errors on the X-coordinate, Y-coordinate, and Z-coordinate of the left condyle were 0.38 ± 0.66 mm (P = .1765), -0.49 ± 0.60 mm (P = .0062), and -0.21 ± 0.43 mm (P = .4307), respectively. When the vertical errors in maxilla involved under-impaction, the mean signed errors on the X-coordinate, Y-coordinate, and Z-coordinate of the left condyle were 0.25 ± 0.83 mm (P = 1.0000), -0.65 ± 0.54 mm (P = .0006), and -0.11 ± 0.65 mm (P = 1.0000), respectively. In subjects with maxillary impaction, the vertical errors in the right and left condyles exhibited no significant difference between over-impaction and under-impaction in the maxilla.

The error patterns of Point B according to vertical errors in the maxilla are described in Table 9 and Figure 12. When the vertical errors in the maxilla involved over-impaction, the mean signed errors on the X-coordinate, Y-coordinate, and Z-coordinate of Point B were 0.26 ± 1.39 mm (P = 1.0000), -0.95 ± 1.19 mm (P

= .0085), and -0.06 ± 1.20 mm (P = 1.0000), respectively. When the vertical errors the maxilla involved under-impaction, the mean signed errors on the X-coordinate, Y-coordinate, and Z-coordinate of Point B were 0.44 ± 0.98 mm (P = 1.0000), -2.11 ± 1.27 mm (P < .0001), and -1.38 ± 1.55 mm (P = .0160), respectively. In subjects with maxillary impaction, the errors in the mandible for under-impaction were significantly downward (P = .0020) and significantly backward (P = .0018) compared to those in the maxilla for over-impaction.

The vertical errors in the maxilla was thought to be one of the factors affecting the surgical accuracy in the distal segment of the mandible.

IV. Discussion

1. Accuracy according to anatomic location

This study analyzed the accuracy of orthognathic surgery by applying a 3D virtual surgical planning system with affine transformation of a rigid body. It was hypothesized that using the virtual planning system would result in negligible surgical errors regardless of any landmarks used in this study. The specific aims of this study were to identify the deviation of landmarks for each segment in three different planes and to visualize those errors using scattergrams. Surgical accuracy aided by virtual surgical planning was achieved in the following order: mandibular condyles, the maxilla, and the distal segment of mandible.

As expected, age and sex were not associated with mean 3D distance errors. Patient age was in a very narrow range (mean age 21 years and 3 months, from 16 years and 11 months to 28 years and 1 months).

The mean 3D distance error was smallest in the right condyle, followed by the left condyle, although the difference as not statistically significant. An error of about 1 mm on average provides stability to the condyle after surgery and the amount of joint movement is reduced to minimize the change in occlusion after surgery.

The maxillary landmarks in this study had similar mean 3D distance error magnitudes of approximately 1.0 mm, and a similar standard deviation of approximately 0.6 mm (Table 4). The right and left condyles had the smallest mean 3D distance errors among all the landmarks. The mean 3D distance errors for the mandibular landmarks increased in the following order: the condyles, mandibular

first molars, L1, and Point B. The standard deviations of the mandibular landmarks also increased in the same order.

Most of the mean signed errors were not significantly different from 0 (Table 5). However, all the mean errors for the condylar landmarks and the landmarks on the distal segment of the mandible for the Y-coordinate were significantly different from 0, and had negative values, which meant errors were in the downward direction. This result was also consistently seen in the scattergrams.

The tendency for the mean signed errors for each anatomic landmark was visualized with scattergrams in this study. The tendency of the errors in both condyles was in the downward and outward directions. It was postulated that upward and inward anatomic boundaries can be a restriction on surgical errors. Additionally, mandibular set back surgery in class III malocclusion had an inherent tendency to increase outward movement for the condyle. This also seemed to be related to interference between the proximal and distal segments of the mandible. However, in the previous study [50], most condyles exhibited linear displacement in the anterior, downward, and inward directions. This may be due to differences in the types of surgery between the present and the previous study: intraoral vertical sagittal ramus osteotomies in the previous study [50] and sagittal split ramus osteotomies in this study.

The errors of the mandible increased in the following order: the condyles, mandibular 1st molars, L1, and Point B (Table 4, Figure 6). Likewise, L1 and Point B errors had greater tendencies to move downward compared to mandibular first molars. Mandibular first molars had larger error ranges than maxillary first molars. This may be related to possible poor adaptation of the surgical splint during temporary intermaxillary fixation. Moreover, several errors occurred in the maxilla,

which included inadequate posterior impaction that could have potentiated the errors in the mandible. Among 52 patients, maxilla posterior impaction with counterclockwise rotation was planned in 41 patients. It seemed that the condyle had fewer tendencies in the magnitude of errors compared to the distal segment of the mandible because of the surrounding soft tissue that held it relatively securely. While the distal segment of the mandible can be influenced by masticatory muscle function, the condyle may act as a rotational center. The greater the distance from the condyle, the more amplified the error in the sagittal plane. The mean signed errors for Point B had a tendency to be backwardly and downwardly located. This may be related to inadequate maxillary repositioning that directed Point B to an excessive clockwise rotation. The mean signed errors for maxillary first molars, Point A, and U1 tended to be slightly forward. This forward tendency in the maxilla may drive the magnitude of errors of the mandible to be more vertical because of occlusal interference produced by cuspal inclinations. It seemed that the maxilla slid forward to avoid interference during temporary intermaxillary fixation when interference by the posterior maxilla was present.

The scattergrams showed that the standard deviations of the landmark errors at the distal segment of the mandible were greater than those of the condylar and maxillary landmarks. Moreover, the contours of the ellipses in the scattergrams were different among the landmarks. The errors for the condyles, the maxilla, and the distal segment of the mandible exhibited different patterns. The errors for the landmarks on the distal segment of the mandible had a wider distribution than those for the condylar and maxillary landmarks. The errors for the distal segment of the mandible seem to be the additive or subtractive result of several factors such as an adaptation

error due to the surgical splint, incorrect posterior impaction of the maxilla, or residual bony interference in multiple directions.

Based on these analyses, possible bone interference should be thoroughly mitigated before bone fixation. Moreover, the operator should be aware of the greater number of errors that occur at the distal segment of the mandible compared to the maxilla. However, in cases of maxillary posterior impactions, it is difficult to identify and eliminate bone interference completely due to poor visibility. Using 3D virtual planning and RP models, it was possible to pre-operatively estimate specific areas where bone interference would occur [31].

The subjects in this study included deformity of facial asymmetry. If patients with more than 4 mm of skeletal menton deviation from the facial midline were categorized as asymmetric [51, 52], 22 subjects comprised the asymmetry group among 52 patients. Six subjects had chin deviated to the right and 16 subjects to the left. The effect of the facial asymmetry on the surgical accuracy was not statistically proved due to the insufficient number of subjects.

2. Accuracy criteria

The accuracy threshold was set at 2 mm for translational measurements according to the standard permitted by previous studies [26-30]. The success criteria in the previous studies were not about mean 3D distance errors, but about errors on the three Cartesian axes. Since the mean absolute errors on the three axes in all the landmarks were less than 2 mm, the results in this study were clinically acceptable according to established criteria. Hsu *et al.* [27] also used a 2 mm threshold, but they suggested a 1 mm threshold for the maxillary dental midline position because it was the most noticeable parameter. The mean absolute error for the X-coordinate in U1 was also less than 1 mm in the present study. Meanwhile, Tucker *et al.* [53] proposed a voxel size threshold, which was 0.5 mm in their study. It seems that the voxel size could be used as the most stringent threshold. However, the voxel size threshold seems to be a technical limitation rather than a clinical guideline. Recently, Borba *et al.* [54] suggested a 1 mm threshold could be used for accuracy assessment for 3D study. However, only vertical axis error (0.76 ± 1.63 mm) and anteroposterior axis error (0.96 ± 1.23 mm) were analyzed, except horizontal axis errors which were unable to be analyzed, in Borba *et al.*'s study. Standard deviations for the vertical and anteroposterior axis errors were greater than 1.0 mm in the study. Borba *et al.* also suggested a 1 mm threshold that consisted of a CBCT 0.5 mm spatial resolution and a 0.5 mm allowance for human mistakes. A more stringent threshold could be used in a 3D accuracy study, unlike a 2D based study. To some extent, consistent with these previous studies, the lower limit of the threshold for the accuracy assessment could be the voxel size, and the threshold for clinical acceptance would be evaluated differently for each segment in a 3D accuracy study. The threshold of

the X-coordinate error in U1 should be more stringent due to esthetics and the threshold of errors in condyles should be more stringent due to post-operative stability. These suggestions are consistent with the result of this study as indicated in Table 4. In the results of this study, the post-operative horizontal position of U1 and Point A were very accurate, 0.64 ± 0.50 mm and 0.66 ± 0.50 mm, respectively, indicating clinically acceptable esthetic results. However, the accuracy at L1 and Point B in the mandible was relatively low, 0.95 ± 0.68 mm and 0.96 ± 0.79 mm, respectively. This range of error as a result of surgery is not considered a significant change that had clinical importance.

3. Comparison with recent studies

Within the limitations of different subjects for each study, comparison with recent studies with respect to the accuracy in orthognathic surgery using virtual planning systems was performed. In recent studies, including the present study, mean linear difference errors were mostly less than 2 mm [29, 55-58]. Student's *t*-tests and Student-Newman-Keuls multiple comparison tests showed that there was no significant difference in mean absolute errors for most landmarks (Table 10). However, the mean absolute errors for the X-coordinates in the maxillary right first molar and Y-coordinates for the maxillary left first molar in the present study were significantly less than those reported in Ritto et al.'s study [26]. Furthermore, the mean absolute error for the Z-coordinates of the maxillary left first molar in the present study was significantly less than that reported in Zhang et al.'s paper [25]. However, the mean absolute error for the L1 X-coordinates in the present study was significantly greater than that in Zhang et al.'s study [25].

In this study, the mean absolute errors were calculated to quantify the magnitude of the errors along three axes, similar to other recent studies [55, 58]. However, De Riu *et al*. [57], Stokbro *et al.* [59], and Chin *et al*. [56] used mean errors, which has the potential to reduce error magnitudes, since positive errors and negative errors cancel each other out in contrast to mean absolute errors.

Errors in the 3D space were measured in this study as done in other recent studies [29, 55, 56, 58]. However, De Riu *et al*. [57] and Ritto *et al.* [30] measured errors only on 2D images projected from 3D CBCTs or 3D CT data. In those studies, it seemed that measurements on 2D projections from 3D objects had inherent limitations and did not take advantage of the 3D analysis.

Chin *et al*. [56] and Zhang *et al*. [29] used additional reference planes during error measurements. In these cases, other errors may have occurred during the establishment of the reference planes. Meanwhile, De Riu *et al*. [57] and Zhang *et al*. [29] did not perform superimpositions. Therefore, they could not directly compare pre-operative planned landmarks with post-operative landmarks and only compared the relative distances of landmarks.

Shaheen *et al*. [58], Ritto *et al*. [30], and Stokbro *et al.* [59] analyzed only maxillary landmarks. Chin *et al.* [56], Zhang *et al*. [29], and Baan *et al*. [55] investigated the maxillary landmarks and the mandibular landmarks of distal segments. Similar to the study by De Riu *et al*. [57], the maxillary landmarks and the mandibular landmarks of distal and proximal segments were analyzed in this study. The condylar area was not investigated in the previous studies. This reasoning is based on a study that found that one of the least reliable landmarks among 3D cephalometric measurements was the mandibular condyle area as reported in a recent systemic

review [60] where various landmarks were evaluated, unlike the reliability of a limited number of 3D cephalometric landmarks reported in previous publications. The errors for condylar landmarks were explicitly analyzed only in this study.

De Riu *et al*. [57], Chin *et al*. [56], and Zhang *et al*. [29] did not investigate the reproducibility of the measurements used in their studies. Reproducibility should be assessed to ascertain measurement reliability. Ritto *et al*. [30] investigated intra-observer reliability and found that ICC showed excellent reliability. In this study, the reliability of superimposition was tested using intra-observer and inter-observer reliabilities, which exhibited excellent ICC results comparable to Shaheen *et al*. [58], Stokbro *et al.* [59, 61], and Baan *et al*.'s studies [55]. Stokbro *et al.* [59, 61] also evaluated the agreement between 2 measurements using Bland-Altman plots. In this study, the agreement among the 3 measurements was analyzed using Bland-Altman plots, which exhibited excellent agreement comparable to Stokbro *et al*.'s study [59, 61].

Similar to Baan *et al*. [55], Shaheen *et al*. [58], and Stokbro *et al*.'s studies [59, 61], the present study has an advantage because the repetitive identification of landmarks is not necessary because of the use of a transformation matrix which provided error results without repetitive landmark identification. Therefore, landmark identification errors were removed from the present study. Baan *et al*. [55] assumed that a virtual triangle consisting of three maxillary tooth landmarks represented the maxilla and another virtual triangle consisting of three mandibular tooth landmarks represented the distal segment of the mandible. Likewise, Shaheen *et al*. [58] and Stokbro *et al*. [59, 61] assumed that an occlusal plane that consisted of three maxillary landmarks or a centroid point calculated from three maxillary landmarks represented the maxilla.

They did not analyze errors for the specific area of the landmarks but only regarded errors for the virtual triangles, the occlusal plane, or the centroid point as the error of the maxilla or the error of the distal segment of the mandible. The errors for the specific parts in the maxilla or mandible may differ from the errors of the maxilla or mandible calculated from the triangles, the occlusal plane, or the centroid point. The errors of the maxilla or mandible could be an additive or subtractive summation of the errors of the specific parts in the maxilla or mandible. In these methods, error analysis of the specific parts in the maxilla and mandible seemed to be impossible since the landmarks were used to construct the transformation matrix [55] or used as input variables for singular value decomposition algorithms [58]. Moreover, they didn't show surgical accuracy for the proximal segment of the mandible. However, in the present study, transformation matrices consisted of the entire movement of the maxilla, the distal segment of the mandible, and the proximal segment of the mandible in 3D space during each superimposition. Therefore, in this study, errors in the individual landmarks can be accurately calculated in any anatomic location.

In Zhang *et al*.'s study [29], the accuracy associated with the maxilla (0.71 mm) was better than the mandible (0.91 mm). This result was consistent with the present study, which showed a similar larger error in the distal segment of the mandible than the maxilla. It seems that errors for the distal segment of the mandible may be more likely to occur than errors in the maxilla since most cases in Zhang *et al*.'s study [29] and all the cases in the present study were patients with skeletal class III malocclusion where mandibular movement was greater than maxillary movement. Zhang *et al*. showed better control in the horizontal direction (0.55 mm) compared to the vertical (0.92 mm) and anteroposterior directions (0.97 mm) for the combined

errors of the maxilla and mandible. Similarly, the present study showed better control in the horizontal (0.76 mm) and anteroposterior directions (0.76 mm) compared to the vertical direction (0.90 mm) for the combined errors of the maxilla and mandible (Table 4). In Baan *et al*.'s study [55], the errors in the maxilla were relatively larger in the vertical (1.85 mm) and the anteroposterior directions (1.41 mm) than in the horizontal direction (0.49 mm). In Ritto *et al*.'s study [30], the errors in the maxilla were relatively larger in the vertical (1.44 mm) than the anteroposterior (0.95 mm) and the horizontal directions (0.90 mm). In Shaheen *et al*.'s study [58], the error of the movement of the maxilla was relatively larger in the anteroposterior (1.2 mm) and the vertical directions (1.1 mm) compared to the horizontal direction (0.8 mm). However, the result of the present study shows that the errors for maxillary movement were relatively larger in the anteroposterior (0.68 mm) and the horizontal directions (0.66 mm) compared to the vertical direction (0.57 mm). The difference in error direction seemed due to the difference in the assessed landmarks. Ritto *et al*. [30] and Shaheen *et al*. [58] only used dental landmarks, while dental landmarks and skeletal landmarks were used in this study. In this study, the direction of maxillary movement was usually upwards and forwards. Therefore, it was possible to measure the amount of maxilla to be resected in a precise manner. Moreover, more accurate osteotomy could be performed on the maxilla with the prediction of bone gaps using the RP model as a reference. Therefore, maxillary vertical errors might be reduced in the present study.

The errors can be seen to be at similar levels between the present study and aforementioned recent studies. The present study includes a larger number of patients compared to other studies. The errors for the condyles were investigated in

the present study in contrast to the other studies which did not assess these. Inappropriate condylar positioning is related to post-operative relapse after orthognathic surgery [62, 63]. The mean absolute errors for the X-coordinate, Y-coordinate, and Z-coordinate, were less than 1.0 mm, and the mean 3D distance errors for the right and left condyles were approximately 1.0 mm and less than the errors for the other landmarks in this study (Table 4). The position of the condyles was the most accurate compared to the other landmarks after surgery, which assures post-operative stability and reduced efforts to realign the dental arch during post-operative orthodontic treatment.

4. Effects of surgical plan for maxilla and error in maxilla

The surgical plans for the maxilla affected the errors in the maxilla and mandible. In cases of maxillary setback, the vertical and anteroposterior errors for Point A and the vertical errors for the right condyle increased significantly compared to cases of maxillary advancement. For the left condyle, there was no significant difference according to the surgical plans for the maxilla. However, in cases of maxillary setback, the mean and standard deviation in the vertical error for the left condyle tended to increase. This is attributed to less setback than the planned position due to interference of the posterior structure when the maxilla is moved backward. The vertical errors in the maxilla did not have significant effects on the errors in the right and left condyles. It is believed that the vertical error in the right and left condyles is affected by the anteroposterior plan for the maxilla rather than the vertical error in the maxilla.

For Point B, the antero-posterior error was significantly higher when the maxilla was moved forward compared to when the maxilla was moved backward. However, it was affected by the vertical error in the maxilla. The vertical and anteroposterior errors significantly increased when the maxilla was less impacted than planned. When the maxillary impaction was less performed than planned, the mandible moved downward and tended to rotate posteriorly. Even when the maxillary impaction was higher than planned, the mandible moved downward, likely due to cuspal interference between the maxillary and mandibular teeth. To determine which factor of the surgical plan for the maxilla and the error in the maxilla has the higher explanatory power to the error for Point B, it is necessary to perform a high-level regression analysis considering the positive and negative numbers. However, the scattergrams imply that the error in the maxilla has greater influence than the surgical plan for the maxilla because when the predictor was the error in the maxilla, the classification seemed to have better performance than when it was the surgical plan for the maxilla.

5. Accurate condylar position

The condyle positions were considered stable since the passive guide for the occlusal splint could be reached at the time of post-operative CBCT taking. During the immediate post-operative admission period, post-operative radiography, including the transcranial view, and the occlusal guide were meticulously checked, and re-fixation surgery was performed when necessary.

The mean 3D distance errors and the standard deviations for the mandibular landmarks increased in the following order: the condyles, mandibular first molars, L1, and Point B (Table 4, Figure 6). There were increasing error magnitudes for landmarks located further from the center of the body axis in the mandible. Another possible reason for fewer errors in the condyle is to relatively loose boxing with the final splint at the post-operative CBCT. This can introduce condylar seating in a comfortable position while potentiating the magnitude of errors in the distal segment of the mandible. Since tight boxing of the splint was applied, the error in the condyle could increase in this study. Although the tight boxing during the post-operative CBCT scan is possible to increase the error in the mandibular condyles, the accuracy among the anatomic locations was highest in the mandibular condyles. This suggests that in the distal segment of the mandible, there may be an error pattern beyond the effect of the tight boxing.

The accuracy of error measurements was improved due to the computational method used for superimposition that was based on a mathematical analysis with affine transformation of a rigid body, which required setting the anatomic landmarks based only on pre-operative 3D data without the need to repetitively identify the landmarks during pre-operative virtual planning or the surgical outcomes. The

system used in this study did not require setting up specific reference planes but directly calculated relative distances in 3D space. Therefore, errors due to establishing and measuring landmark distance from the reference planes could be effectively excluded.

The condylar landmarks were investigated in this study since it is clinically relevant in terms of post-postoperative stability. Compared to the conventional method, 3D virtual surgical planning eliminates the need for dental impressions and simplifies the technical steps [64]. The analysis that assessed the efficiency of planning for bi-maxillary orthognathic surgery showed that virtual planning effectively reduced planning time up to 60 minutes on average compared to the conventional method [65]. Virtual planning based on 3D technologies can improve surgical outcomes by accurately estimating the final results of orthognathic surgery because of the elimination of potential errors related to 2D paper surgery planning and dental model mounting with facebow transfers through virtual planning.

V. Conclusions

The computational method for one-time landmark setting exhibited excellent agreement among the measurements. This method can be applied reliably for evaluation of surgical outcomes in orthognathic surgery. Surgical accuracy aided by virtual surgical planning was achieved in the following order: the mandibular right and left condyles, maxilla, and the distal segment of the mandible. The accuracy was affected by the surgical plan for the maxilla and the error in the maxilla. Surgeons should be aware of the possibility of errors in the distal segment of the mandible, which is potentiated by an incorrect maxillary position. More attention should be paid to reduce surgical errors that occur in the posterior maxilla, which might not be clearly visualized during orthognathic surgery.

References

1. Meger MN, Fatturi AL, Gerber JT, Weiss SG, Rocha JS, Scariot R, et al. Impact of orthognathic surgery on quality of life of patients with dentofacial deformity: a systematic review and meta-analysis. Br J Oral Maxillofac Surg. 2021;59(3):265-271.
2. Proothi M, Drew SJ, Sachs SA. Motivating factors for patients undergoing orthognathic surgery evaluation. J Oral Maxillofac Surg. 2010;68(7):1555-1559.
3. Stokbro K, Aagaard E, Torkov P, Bell RB, Thygesen T. Virtual planning in orthognathic surgery. Int J Oral Maxillofac Surg. 2014;43(8):957-965.
4. Zizelmann C, Hammer B, Gellrich NC, Schwestka-Polly R, Rana M, Bucher P. An evaluation of face-bow transfer for the planning of orthognathic surgery. J Oral Maxillofac Surg. 2012;70(8):1944-1950.
5. Berco M, Rigali PH, Jr., Miner RM, DeLuca S, Anderson NK, Will LA. Accuracy and reliability of linear cephalometric measurements from cone-beam computed tomography scans of a dry human skull. Am J Orthod Dentofacial Orthop. 2009;136(1):17.e11-19.
6. Park SY, Hwang DS, Song JM, Kim UK. Comparison of time and cost between conventional surgical planning and virtual surgical planning in orthognathic surgery in Korea. Maxillofac Plast Reconstr Surg. 2019;41(1):35.
7. Barbenel JC, Paul PE, Khambay BS, Walker FS, Moos KF, Ayoub AF. Errors in orthognathic surgery planning: the effect of inaccurate study model orientation. Int J Oral Maxillofac Surg. 2010;39(11):1103-1108.
8. Sun Y, Luebbers HT, Agbaje JO, Schepers S, Vrielinck L, Lambrichts I, et al. Accuracy of upper jaw positioning with intermediate splint fabrication after virtual planning in bimaxillary orthognathic surgery. J Craniofac Surg. 2013;24(6):1871-1876.
9. Kwon TG, Choi JW, Kyung HM, Park HS. Accuracy of maxillary repositioning in two-jaw surgery with conventional articulator model

surgery versus virtual model surgery. Int J Oral Maxillofac Surg. 2014;43(6):732-738.

10. Haas OL, Jr., Becker OE, de Oliveira RB. Computer-aided planning in orthognathic surgery-systematic review. Int J Oral Maxillofac Surg. 2015;44(3):329-342.
11. Levine JP, Patel A, Saadeh PB, Hirsch DL. Computer-aided design and manufacturing in craniomaxillofacial surgery: the new state of the art. J Craniofac Surg. 2012;23(1):288-293.
12. Swennen GR, Mollemans W, Schutyser F. Three-dimensional treatment planning of orthognathic surgery in the era of virtual imaging. J Oral Maxillofac Surg. 2009;67(10):2080-2092.
13. Lin HH, Lonic D, Lo LJ. 3D printing in orthognathic surgery - A literature review. J Formos Med Assoc. 2018;117(7):547-558.
14. Adolphs N, Liu W, Keeve E, Hoffmeister B. RapidSplint: virtual splint generation for orthognathic surgery - results of a pilot series. Comput Aided Surg. 2014;19(1-3):20-28.
15. Stokbro K, Aagaard E, Torkov P, Bell RB, Thygesen T. Surgical accuracy of three-dimensional virtual planning: a pilot study of bimaxillary orthognathic procedures including maxillary segmentation. Int J Oral Maxillofac Surg. 2016;45(1):8-18.
16. Chen Z, Mo S, Fan X, You Y, Ye G, Zhou N. A Meta-analysis and Systematic Review Comparing the Effectiveness of Traditional and Virtual Surgical Planning for Orthognathic Surgery: Based on Randomized Clinical Trials. J Oral Maxillofac Surg. 2021;79(2):471.e1-471.e19.
17. Gaber RM, Shaheen E, Falter B, Araya S, Politis C, Swennen GRJ, et al. A Systematic Review to Uncover a Universal Protocol for Accuracy Assessment of 3-Dimensional Virtually Planned Orthognathic Surgery. J Oral Maxillofac Surg. 2017;75(11):2430-2440.
18. Plooij JM, Maal TJ, Haers P, Borstlap WA, Kuijpers-Jagtman AM, Berge SJ. Digital three-dimensional image fusion processes for planning and evaluating orthodontics and orthognathic surgery. A systematic review. Int J Oral Maxillofac Surg. 2011;40(4):341-352.

19. Hajeer MY, Mao Z, Millett DT, Ayoub AF, Siebert JP. A new three-dimensional method of assessing facial volumetric changes after orthognathic treatment. Cleft Palate Craniofac J. 2005;42(2):113-120.
20. Zinser MJ, Mischkowski RA, Sailer HF, Zoller JE. Computer-assisted orthognathic surgery: feasibility study using multiple CAD/CAM surgical splints. Oral Surg Oral Med Oral Pathol Oral Radiol. 2012;113(5):673-687.
21. Shamir RR, Freiman M, Joskowicz L, Spektor S, Shoshan Y. Surface-based facial scan registration in neuronavigation procedures: a clinical study. J Neurosurg. 2009;111(6):1201-1206.
22. Cevidanes LH, Bailey LJ, Tucker GR, Jr., Styner MA, Mol A, Phillips CL, et al. Superimposition of 3D cone-beam CT models of orthognathic surgery patients. Dentomaxillofac Radiol. 2005;34(6):369-375.
23. Nada RM, Maal TJ, Breuning KH, Berge SJ, Mostafa YA, Kuijpers-Jagtman AM. Accuracy and reproducibility of voxel based superimposition of cone beam computed tomography models on the anterior cranial base and the zygomatic arches. PLoS One. 2011;6(2):e16520.
24. Ghoneima A, Cho H, Farouk K, Kula K. Accuracy and reliability of landmark-based, surface-based and voxel-based 3D cone-beam computed tomography superimposition methods. Orthod Craniofac Res. 2017;20(4):227-236.
25. Almukhtar A, Ju X, Khambay B, McDonald J, Ayoub A. Comparison of the accuracy of voxel based registration and surface based registration for 3D assessment of surgical change following orthognathic surgery. PLoS One. 2014;9(4):e93402.
26. Kaipatur N, Al-Thomali Y, Flores-Mir C. Accuracy of computer programs in predicting orthognathic surgery hard tissue response. J Oral Maxillofac Surg. 2009;67(8):1628-1639.
27. Hsu SS, Gateno J, Bell RB, Hirsch DL, Markiewicz MR, Teichgraeber JF, et al. Accuracy of a computer-aided surgical simulation protocol for orthognathic surgery: a prospective multicenter study. J Oral Maxillofac Surg. 2013;71(1):128-142.
28. Schouman T, Rouch P, Imholz B, Fasel J, Courvoisier D, Scolozzi P.

Accuracy evaluation of CAD/CAM generated splints in orthognathic surgery: a cadaveric study. Head Face Med. 2015;11:24.

29. Zhang N, Liu S, Hu Z, Hu J, Zhu S, Li Y. Accuracy of virtual surgical planning in two-jaw orthognathic surgery: comparison of planned and actual results. Oral Surg Oral Med Oral Pathol Oral Radiol. 2016;122(2):143-151.
30. Ritto FG, Schmitt ARM, Pimentel T, Canellas JV, Medeiros PJ. Comparison of the accuracy of maxillary position between conventional model surgery and virtual surgical planning. Int J Oral Maxillofac Surg. 2018;47(2):160-166.
31. Lee YC, Sohn HB, Kim SK, Bae OY, Lee JH. A novel method for the management of proximal segment using computer assisted simulation surgery: correct condyle head positioning and better proximal segment placement. Maxillofac Plast Reconstr Surg. 2015;37(1):21.
32. Weissheimer A, Menezes LM, Koerich L, Pham J, Cevidanes LH. Fast three-dimensional superimposition of cone beam computed tomography for orthopaedics and orthognathic surgery evaluation. Int J Oral Maxillofac Surg. 2015;44(9):1188-1196.
33. Xia Z, Huang X, Zhou X, Sun Y, Ntziachristos V, Wong ST. Registration of 3-D CT and 2-D flat images of mouse via affine transformation. IEEE Trans Inf Technol Biomed. 2008;12(5):569-578.
34. Domokos C, Kato Z. Realigning 2D and 3D Object Fragments without Correspondences. IEEE Trans Pattern Anal Mach Intell. 2016;38(1):195-202.
35. Besl PJ, McKay ND. A method for registration of 3-D shapes. IEEE Trans Pattern Anal Mach Intell. 1992;14(2):239-256.
36. Mazur J, Jernigan RL. Comparison of rotation models for describing DNA conformations: application to static and polymorphic forms. Biophys J. 1995;68(4):1472-1489.
37. Parker JG, Mair BA, Gilland DR. Respiratory motion correction in gated cardiac SPECT using quaternion-based, rigid-body registration. Med Phys. 2009;36(10):4742-4754.
38. Schreiner W, Karch R, Ribarics R, Cibena M, Ilieva N. Relative Movements

of Domains in Large Molecules of the Immune System. J Immunol Res. 2015;2015:210675.

39. Kang TJ, Eo SH, Cho H, Donatelli RE, Lee SJ. A sparse principal component analysis of Class III malocclusions. Angle Orthod. 2019;89(5):768-774.

40. R Development Core Team. R: A language and environment for statistical computing. Vienna, Austria: R Foundation for Statistical Computing; 2019.

41. de Vet HCW, Terwee CB, Knol DL, Bouter LM. When to use agreement versus reliability measures. J Clin Epidemiol. 2006;59(10):1033-1039.

42. Costa-Santos C, Bernardes J, Ayres-de-Campos D, Costa A, Costa C. The limits of agreement and the intraclass correlation coefficient may be inconsistent in the interpretation of agreement. J Clin Epidemiol. 2011;64(3):264-269.

43. Kottner J, Audige L, Brorson S, Donner A, Gajewski BJ, Hrobjartsson A, et al. Guidelines for Reporting Reliability and Agreement Studies (GRRAS) were proposed. J Clin Epidemiol. 2011;64(1):96-106.

44. McGraw KO, Wong SP. Forming inferences about some intraclass correlation coefficients. Psychol Methods. 1996;1(1):30-46.

45. Koo TK, Li MY. A Guideline of Selecting and Reporting Intraclass Correlation Coefficients for Reliability Research. J Chiropr Med. 2016;15(2):155-163.

46. Bland JM, Altman DG. Statistical methods for assessing agreement between two methods of clinical measurement. Lancet. 1986;1(8476):307-310.

47. Park J, Baumrind S, Curry S, Carlson SK, Boyd RL, Oh H. Reliability of 3D dental and skeletal landmarks on CBCT images. Angle Orthod. 2019;89(5):758-767.

48. Donatelli RE, Lee SJ. How to report reliability in orthodontic research: Part 1. Am J Orthod Dentofacial Orthop. 2013;144(1):156-161.

49. Donatelli RE, Lee SJ. How to report reliability in orthodontic research: Part 2. Am J Orthod Dentofacial Orthop. 2013;144(2):315-318.

50. Han YS, Jung YE, Song IS, Lee SJ, Seo BM. Three-Dimensional Computed Tomographic Assessment of Temporomandibular Joint Stability After Orthognathic Surgery. J Oral Maxillofac Surg. 2016;74(7):1454-1462.

51. Haraguchi S, Takada K, Yasuda Y. Facial asymmetry in subjects with skeletal Class III deformity. Angle Orthod. 2002;72(1):28-35.
52. Masuoka N, Muramatsu A, Ariji Y, Nawa H, Goto S, Ariji E. Discriminative thresholds of cephalometric indexes in the subjective evaluation of facial asymmetry. Am J Orthod Dentofacial Orthop. 2007;131(5):609-613.
53. Tucker S, Cevidanes LH, Styner M, Kim H, Reyes M, Proffit W, et al. Comparison of actual surgical outcomes and 3-dimensional surgical simulations. J Oral Maxillofac Surg. 2010;68(10):2412-2421.
54. Borba AM, Jose da Silva E, Fernandes da Silva AL, Han MD, da Graca Naclerio-Homem M, Miloro M. Accuracy of Orthognathic Surgical Outcomes Using 2- and 3-Dimensional Landmarks-The Case for Apples and Oranges? J Oral Maxillofac Surg. 2018;76(8):1746-1752.
55. Baan F, Liebregts J, Xi T, Schreurs R, de Koning M, Berge S, et al. A New 3D Tool for Assessing the Accuracy of Bimaxillary Surgery: The OrthoGnathicAnalyser. PLoS One. 2016;11(2):e0149625.
56. Chin SJ, Wilde F, Neuhaus M, Schramm A, Gellrich NC, Rana M. Accuracy of virtual surgical planning of orthognathic surgery with aid of CAD/CAM fabricated surgical splint-A novel 3D analyzing algorithm. J Craniomaxillofac Surg. 2017;45(12):1962-1970.
57. De Riu G, Virdis PI, Meloni SM, Lumbau A, Vaira LA. Accuracy of computer-assisted orthognathic surgery. J Craniomaxillofac Surg. 2018;46(2):293-298.
58. Shaheen E, Shujaat S, Saeed T, Jacobs R, Politis C. Three-dimensional planning accuracy and follow-up protocol in orthognathic surgery: a validation study. Int J Oral Maxillofac Surg. 2019;48(1):71-76.
59. Stokbro K, Thygesen T. Surgical Accuracy in Inferior Maxillary Reposition. J Oral Maxillofac Surg. 2018;76(12):2618-2624.
60. Sam A, Currie K, Oh H, Flores-Mir C, Lagravere-Vich M. Reliability of different three-dimensional cephalometric landmarks in cone-beam computed tomography : A systematic review. Angle Orthod. 2019;89(2):317-332.
61. Stokbro K, Thygesen T. A 3-Dimensional Approach for Analysis in

Orthognathic Surgery-Using Free Software for Voxel-Based Alignment and Semiautomatic Measurement. J Oral Maxillofac Surg. 2018;76(6):1316-1326.

62. Kim YJ, Lee Y, Chun YS, Kang N, Kim SJ, Kim M. Condylar positional changes up to 12 months after bimaxillary surgery for skeletal class III malocclusions. J Oral Maxillofac Surg. 2014;72(1):145-156.

63. Hoppenreijs TJ, Maal T, Xi T. Evaluation of Condylar Resorption Before and After Orthognathic Surgery. Seminars in Orthodontics. 2013;19(2):106-115.

64. Hernandez-Alfaro F, Guijarro-Martinez R. New protocol for three-dimensional surgical planning and CAD/CAM splint generation in orthognathic surgery: an in vitro and in vivo study. Int J Oral Maxillofac Surg. 2013;42(12):1547-1556.

65. Schwartz HC. Does computer-aided surgical simulation improve efficiency in bimaxillary orthognathic surgery? Int J Oral Maxillofac Surg. 2014;43(5):572-576.

Tables

Table 1. Anatomic location and landmarks

Anatomic location	Landmark	Definition
Mandible, right proximal segment	Right condyle	The midpoint of the rectangles formed by the tangent lines around the right condyle head
Mandible, left proximal segment	Left condyle	The midpoint of the rectangles formed by the tangent lines around the left condyle head
Maxilla	#16	The mesiobuccal cusp tip of the upper right 1st molar
	#26	The mesiobuccal cusp tip of the upper left 1st molar
	Point A	The most concave point on the sagittal plane between the anterior nasal spine and the upper incisal alveolus
	U1	The midpoint between the midpoint of the incisal edge of the upper right central incisor and the midpoint of the incisal edge of the upper left central incisor
Mandible, distal segment	#36	The mesiobuccal cusp tip of the lower left 1st molar
	#46	The mesiobuccal cusp tip of the lower right 1st molar
	L1	The midpoint between the midpoint of the incisal edge of the lower right central incisor and the midpoint of the incisal edge of the lower left central incisor
	Point B	The most concave point on the sagittal between the pogonion and the lower incisal alveolus

Table 2. Descriptive summary of study subjects

Study Variable	Value[a]
Number of subjects	52 (100%)
Age (year)	21.3 [16.9, 28.1]
Sex	
Female	26 (50%)
Male	26 (50%)
Dentofacial deformity	
Skeletal class III malocclusion	52 (100%)
Surgical plan	
Maxilla	
Vertical	
Impaction	48 (92.31%)
No movement	1 (0.02%)
Elongation	3 (0.06%)
Anteroposterior	
Advancement	32 (61.54%)
Setback	20 (38.46%)
Mandible, distal segment	
Vertical	
Impaction	52 (100%)
Anteroposterior	
Setback	52 (100%)

[a] Data presented as number (percentage) or mean [minimum, maximum].

Table 3. Intra-observer and inter-observer reliability according to the intraclass correlation coefficients (ICC)

Landmark	Intra-observer ICC			Inter-observer ICC		
	X-coordinate (horizontal)	Y-coordinate (vertical)	Z-coordinate (anteroposterior)	X-coordinate (horizontal)	Y-coordinate (vertical)	Z-coordinate (anteroposterior)
Right condyle	0.9985	0.9966	0.9962	0.9982	0.9910	0.9897
Left condyle	0.9991	0.9990	0.9974	0.9987	0.9975	0.9923
#16	0.9998	0.9992	0.9999	0.9994	0.9987	0.9991
#26	0.9997	0.9997	0.9999	0.9994	0.9987	0.9996
Point A	0.9990	0.9994	0.9999	0.9987	0.9976	0.9997
U1	0.9997	0.9995	0.9999	0.9991	0.9978	0.9993
#36	1.0000	0.9999	1.0000	0.9999	0.9997	0.9999
#46	1.0000	0.9994	0.9999	0.9999	0.9990	0.9999
L1	1.0000	0.9997	1.0000	0.9999	0.9994	0.9999
Point B	1.0000	0.9997	1.0000	0.9999	0.9995	1.0000

Table 4. Mean three-dimensional (3D) distance errors and mean absolute errors

Landmark	Mean 3D distance error[a]	Mean absolute error [b]		
		X-coordinate (horizontal)	Y-coordinate (vertical)	Z-coordinate (anteroposterior)
A. Mandible, proximal segment				
Right condyle	0.95 ± 0.68	0.49 ± 0.43	0.51 ± 0.53	0.45 ± 0.45
Left condyle	1.12 ± 0.62	0.58 ± 0.52	0.66 ± 0.54	0.44 ± 0.32
Total	1.03 ± 0.65	0.54 ± 0.48	0.59 ± 0.54	0.44 ± 0.39
B. Maxilla				
#16	1.33 ± 0.61	0.67 ± 0.48	0.56 ± 0.55	0.75 ± 0.54
#26	1.17 ± 0.60	0.68 ± 0.48	0.46 ± 0.42	0.66 ± 0.46
Point A	1.19 ± 0.56	0.66 ± 0.50	0.58 ± 0.48	0.57 ± 0.42
U1	1.32 ± 0.64	0.64 ± 0.50	0.67 ± 0.50	0.74 ± 0.50
Total	1.25 ± 0.60	0.66 ± 0.49	0.57 ± 0.49	0.68 ± 0.48
C. Mandible, distal segment				
#36	1.96 ± 0.97	0.97 ± 0.78	1.07 ± 0.93	0.87 ± 0.69
#46	2.11 ± 1.09	0.97 ± 0.78	1.22 ± 0.99	1.01 ± 0.78
L1	2.34 ± 1.16	0.95 ± 0.68	1.67 ± 1.22	0.84 ± 0.69
Point B	2.55 ± 1.32	0.96 ± 0.79	1.62 ± 1.19	1.27 ± 1.03
Total	2.24 ± 1.15	0.96 ± 0.76	1.40 ± 1.11	1.00 ± 0.82
A + C	1.84 ± 1.16	0.82 ± 0.70	1.13 ± 1.03	0.81 ± 0.75
A + B + C	1.60 ± 1.02	0.76 ± 0.63	0.90 ± 0.90	0.76 ± 0.66

[a,b] Data presented as mean ± standard deviation in millimeter unit. *P* value for each landmark from the *t*-tests with the Bonferroni correction was less than .0001.

[a] The null hypothesis was that the mean 3D distance error was 0 for each landmark.

[b] The null hypothesis was that the mean absolute error was 0 for each landmark.

Table 5. Mean signed errors

Landmark	Mean signed error[a] (*P* Value[b])		
	X-coordinate (horizontal)	Y-coordinate (vertical)	Z-coordinate (anteroposterior)
A. Mandible, proximal segment			
Right condyle	-0.23 ± 0.61 (.4012)	-0.42 ± 0.61 (.0004*)	-0.09 ± 0.63 (1.0000)
Left condyle	0.32 ± 0.71 (.0907)	-0.57 ± 0.64 (< .0001*)	-0.17 ± 0.52 (1.0000)
Total	0.05 ± 0.72 (1.0000)	-0.49 ± 0.63 (< .0001*)	-0.13 ± 0.58 (1.0000)
B. Maxilla			
#16	-0.06 ± 0.83 (1.0000)	-0.02 ± 0.79 (1.0000)	0.34 ± 0.86 (.2584)
#26	-0.06 ± 0.84 (1.0000)	0.15 ± 0.61 (1.0000)	0.21 ± 0.78 (1.0000)
Point A	-0.06 ± 0.83 (1.0000)	0.08 ± 0.75 (1.0000)	0.27 ± 0.65 (.2225)
U1	0.03 ± 0.82 (1.0000)	0.08 ± 0.84 (1.0000)	0.29 ± 0.85 (.7850)
Total	-0.04 ± 0.82 (1.0000)	0.07 ± 0.75 (1.0000)	0.28 ± 0.79 (< .0001*)
C. Mandible, distal segment			
#36	0.17 ± 1.24 (1.0000)	-0.89 ± 1.11 (< .0001*)	0.04 ± 1.12 (1.0000)
#46	0.18 ± 1.24 (1.0000)	-1.05 ± 1.17 (< .0001*)	0.14 ± 1.28 (1.0000)
L1	0.25 ± 1.15 (1.0000)	-1.56 ± 1.36 (< .0001*)	0.00 ± 1.09 (1.0000)
Point B	0.33 ± 1.21 (1.0000)	-1.50 ± 1.34 (< .0001*)	-0.62 ± 1.52 (.2247)
Total	0.23 ± 1.20 (.2776)	-1.25 ± 1.27 (< .0001*)	-0.11 ± 1.29 (1.0000)
A + C	0.17 ± 1.07 (.2492)	-1.00 ± 1.16 (< .0001*)	-0.12 ± 1.10 (1.0000)
A + B + C	0.09 ± 0.98 (1.0000)	-0.57 ± 1.14 (< .0001*)	0.04 ± 1.01 (1.0000)

[a] Data presented as mean ± standard deviation in millimeter unit.

[b] Results from the *t*-tests with the Bonferroni correction. The null hypothesis was that the mean signed error was 0 for each landmark.

* Statistically significant ($P < .05$).

Table 6. Bivariate analyses of the age, sex and anatomic location with the mean three-dimensional (3D) distance error

Study variable	Mean 3D distance error[a]	95% Confidence interval[b]	*P* Value
Age	β = 0.04	(-0.0019, 0.0779)	.0620
Sex			.1660
Female	1.54 ± 0.95	Reference	
Male	1.67 ± 1.08	(-0.0514, 0.2992)	
Anatomic location			< .0001*[c]
Right condyle	0.95 ± 0.68	Reference	
Left condyle	1.12 ± 0.62	(-0.1744, 0.4989)	
Maxilla	1.25 ± 0.60	(0.0328, 0.5651)	
Mandible, distal segment	2.24 ± 1.15	(1.0204, 1.5528)	

[a] Data presented as mean ± standard deviation (mm) or β, regression coefficient (mm/year).

[b] Data presented as (lower limit, upper limit) in millimeter unit.

[c] Result of one-way ANOVA. The null hypothesis was that the mean 3D distance error was not different according to the anatomic location.

* Statistically significant ($P < .05$).

Table 7. Multiple linear regression model for the mean three-dimensional distance error

Study variable	β	95% Confidence interval[a]	*P* value	Difference by additional analyses
Age	0.03[b]	(-0.0036, 0.0683)	.0774	
Sex				
Female	Reference			
Male	0.08[c]	(-0.0774, 0.2379)	.3180	
Anatomic location				
Right condyle	Reference			
Left condyle	0.16[c]	(-0.1732, 0.4977)	.3425	
Maxilla	0.30[c]	(0.0337, 0.5641)	.0272*	Maxilla > Right condyle[d]
Mandible, distal segment	1.29[c]	(1.0214, 1.5518)	< .0001*	Mandible, distal segment > Maxilla[e], Mandible, distal segment > Left condyle[e], Mandible, distal segment > Right condyle[e]

Abbreviations: β, regression coefficients.

[a] Data presented as (lower limit, upper limit) in millimeter unit.

[b] The unit is mm/year.

[c] The unit is mm/reference.

[d] Results from the same multiple linear regression analysis with the reference of the anatomic location set to the maxilla ($P = .0272$).

[e] Results from the same multiple linear regression analysis with the reference of the anatomic location set to the distal segment of the mandible ($P < .0001$).

* Statistically significant ($P < .05$).

Table 8. Mean signed errors according to surgical plans for the maxilla

Landmark	Surgical plan for the maxilla[a]		Number of subjects	Mean signed error[b] (*P* Value[c])		
	Vertical	Anteroposterior		X-coordinate (horizontal)	Y-coordinate (vertical)	Z-coordinate (anteroposterior)
Point A	Impaction	Total	48	-0.05 ± 0.85 (1.0000)	0.08 ± 0.78 (1.0000)	0.25 ± 0.68 (.4367)
		Advancement	29	0.00 ± 0.91 (1.0000)	-0.16 ± 0.74 (1.0000)	0.05 ± 0.70 (1.0000)
		Setback	19	-0.12 ± 0.78 (1.0000)	0.46 ± 0.69 (.3470)	0.57 ± 0.51 (.0047*)
		P value[d]		.6331	.0054*	.0080*
Right condyle	Impaction	Total	48	-0.22 ± 0.60 (.5447)	-0.40 ± 0.61 (.0014*)	-0.07 ± 0.65 (1.0000)
		Advancement	29	-0.24 ± 0.46 (.3285)	-0.17 ± 0.37 (.7362)	-0.21 ± 0.49 (1.0000)
		Setback	19	-0.18 ± 0.77 (1.0000)	-0.76 ± 0.74 (.0105*)	0.13 ± 0.81 (1.0000)
		P value[d]		.7773	.0035*	.1185
Left condyle	Impaction	Total	48	0.32 ± 0.74 (.1440)	-0.56 ± 0.58 (< .0001*)	-0.17 ± 0.54 (1.0000)
		Advancement	29	0.33 ± 0.76 (.9986)	-0.44 ± 0.47 (.0011*)	-0.19 ± 0.57 (1.0000)
		Setback	19	0.31 ± 0.71 (1.0000)	-0.76 ± 0.67 (.0041*)	-0.14 ± 0.50 (1.0000)
		P value[d]		.9386	.0597	.7514
Point B	Impaction	Total	48	0.34 ± 1.22 (1.0000)	-1.46 ± 1.34 (< .0001*)	-0.64 ± 1.50 (.1847)
		Advancement	29	0.45 ± 1.37 (1.0000)	-1.72 ± 1.44 (< .0001*)	-1.10 ± 1.45 (.0123*)
		Setback	19	0.16 ± 0.95 (1.0000)	-1.06 ± 1.09 (.0182*)	0.06 ± 1.34 (1.0000)
		P value[d]		.4248	.0988	.0075*

[a] Average surgical plan of U1, Point A, #16, and #26.

[b] Data presented as mean ± standard deviation in millimeter unit.

[c] Results from the *t*-tests with the Bonferroni correction. The null hypothesis was that the mean signed error was 0.

[d] Results from the *t*-tests. The null hypothesis was that the difference between the mean signed errors for the advancement and setback was 0.

* Statistically significant ($P < .05$).

Table 9. Mean signed errors according to errors in the maxilla

Landmark	Surgical plan for the maxilla[a]	Error in the maxilla[b]	Number of subjects	Mean signed error[c] (*P* Value[d])		
	Vertical	Vertical		X-coordinate (horizontal)	Y-coordinate (vertical)	Z-coordinate (anteroposterior)
Right condyle	Impaction	Total	48	-0.22 ± 0.60 (.4085)	-0.40 ± 0.61 (.0010*)	-0.07 ± 0.65 (1.0000)
		Over-impaction[e]	27	-0.30 ± 0.61 (.4992)	-0.55 ± 0.63 (.0033*)	-0.03 ± 0.60 (1.0000)
		Under-impaction[f]	21	-0.11 ± 0.57 (1.0000)	-0.21 ± 0.54 (1.0000)	-0.12 ± 0.72 (1.0000)
		P Value[g]		.2960	.0554	.6362
Left condyle	Impaction	Total	48	0.32 ± 0.74 (.1080)	-0.56 ± 0.58 (< .0001*)	-0.17 ± 0.54 (.9534)
		Over-impaction[e]	27	0.38 ± 0.66 (.1765)	-0.49 ± 0.60 (.0062*)	-0.21 ± 0.43 (.4307)
		Under-impaction[f]	21	0.25 ± 0.83 (1.0000)	-0.65 ± 0.54 (.0006*)	-0.11 ± 0.65 (1.0000)
		P Value[g]		.5669	.3556	.5229
Point B	Impaction	Total	48	0.34 ± 1.22 (1.0000)	-1.46 ± 1.34 (< .0001*)	-0.64 ± 1.50 (.1385)
		Over-impaction[e]	27	0.26 ± 1.39 (1.0000)	-0.95 ± 1.19 (.0085*)	-0.06 ± 1.20 (1.0000)
		Under-impaction[f]	21	0.44 ± 0.98 (1.0000)	-2.11 ± 1.27 (< .0001*)	-1.38 ± 1.55 (.0160*)
		P Value[g]		.6308	.0020*	.0018*

[a] Average surgical plan of U1, Point A, #16, and #26.

[b] Average error of U1, Point A, #16, and #26.

[c] Data presented as mean ± standard deviation in millimeter unit.

[d] Results from the *t*-tests with the Bonferroni correction. The null hypothesis was that the mean signed error was 0.

[e] Cases in which the amount of the maxillary impaction was larger than the planned.

[f] Cases in which the amount of the maxillary impaction was smaller than the planned.

[g] Results from the *t*-tests. The null hypothesis was that the difference between the mean signed errors for the over-impaction and under-impaction was 0.

* Statistically significant ($P < .05$).

Table 10. Statistical comparison with recent studies

Landmark	Coordinate	Mean absolute error[a]			Test	Result
		This study	Ritto *et al*. [30]	Zhang *et al*. [29]		
#16	X	0.67 ± 0.48	1.18 ± 0.61	0.8 ± 0.4	SNK	N/S except MAE in this study < MAE in Ritto *et al*.*
	Y	0.56 ± 0.55	0.96 ± 0.89	0.6 ± 0.2	SNK	N/S
	Z	0.75 ± 0.54	N/A	0.9 ± 0.3	Student's *t*	N/S
#26	X	0.68 ± 0.48	0.74 ± 0.89	0.5 ± 0.2	SNK	N/S
	Y	0.46 ± 0.42	1.62 ± 1.57	0.7 ± 0.3	SNK	N/S except MAE in this study < MAE in Ritto *et al*.* and MAE in Zhang *et al*. < MAE in Ritto *et al*.*
	Z	0.66 ± 0.46	N/A	1.0 ± 0.5	Student's *t*	MAE in this study < MAE in Zhang *et al*.*
U1	X	0.64 ± 0.50	N/A	0.4 ± 0.1	Student's *t*	N/S
	Y	0.67 ± 0.50	N/A	0.7 ± 0.3	Student's *t*	N/S
	Z	0.74 ± 0.50	N/A	0.8 ± 0.4	Student's *t*	N/S
#36	X	0.97 ± 0.78	N/A	0.6 ± 0.3	Student's *t*	N/S
	Y	1.07 ± 0.93	N/A	1.2 ± 0.5	Student's *t*	N/S
	Z	0.87 ± 0.69	N/A	1.0 ± 0.5	Student's *t*	N/S
#46	X	0.97 ± 0.78	N/A	0.7 ± 0.3	Student's *t*	N/S
	Y	1.22 ± 0.99	N/A	1.0 ± 0.4	Student's *t*	N/S
	Z	1.01 ± 0.78	N/A	1.1 ± 0.6	Student's *t*	N/S
L1	X	0.95 ± 0.68	N/A	0.5 ± 0.3	Student's *t*	MAE in Zhang *et al*. < MAE in this study*
	Y	1.67 ± 1.22	N/A	1.1 ± 0.5	Student's *t*	N/S
	Z	0.84 ± 0.69	N/A	1.0 ± 0.4	Student's *t*	N/S

Abbreviations: SNK, Student-Newman-Keuls; N/S, No significant difference; MAE, Mean absolute error; N/A, Not applicable.

[a] Data presented as mean ± standard deviation in millimeter unit.

* Statistically significant ($P < .05$).

Figures

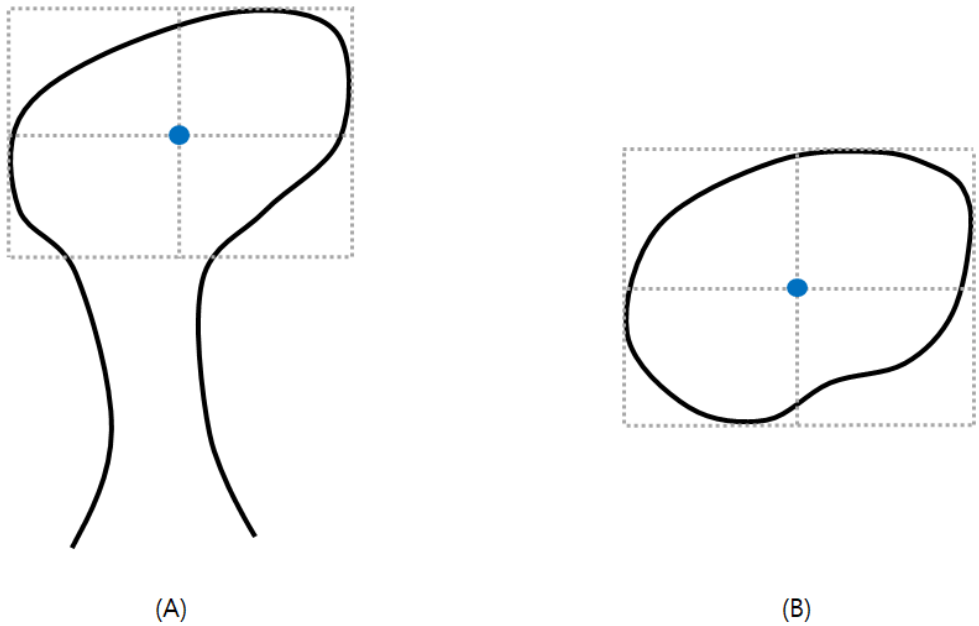

Figure 1. The landmark of the condyle. **(A)** The midpoint in the coronal plane. **(B)** The midpoint in the axial plane.

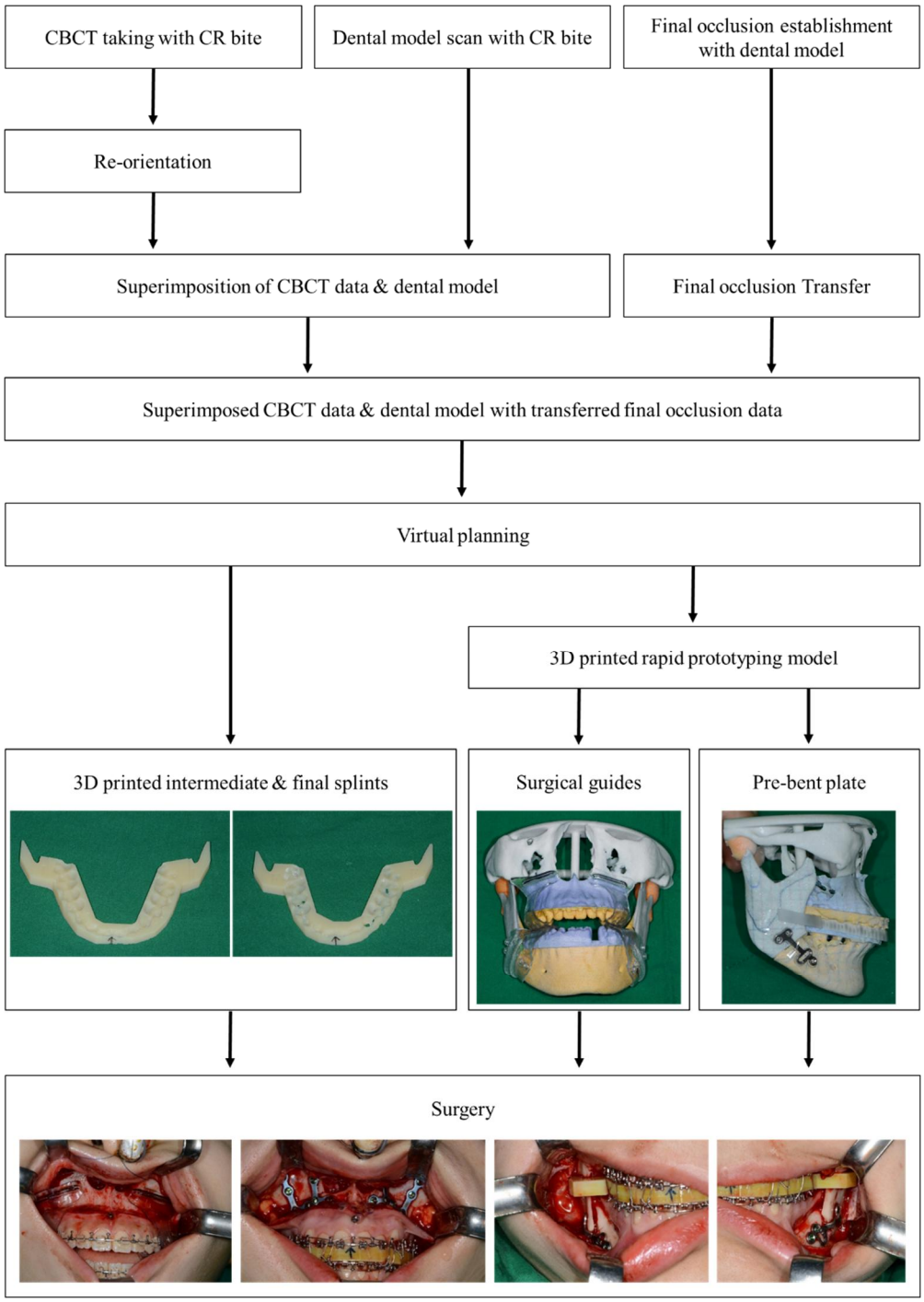

Figure 2. The workflow of virtual surgical planning.

Abbreviations: CR, centric relation; CBCT, cone beam computerized tomography.

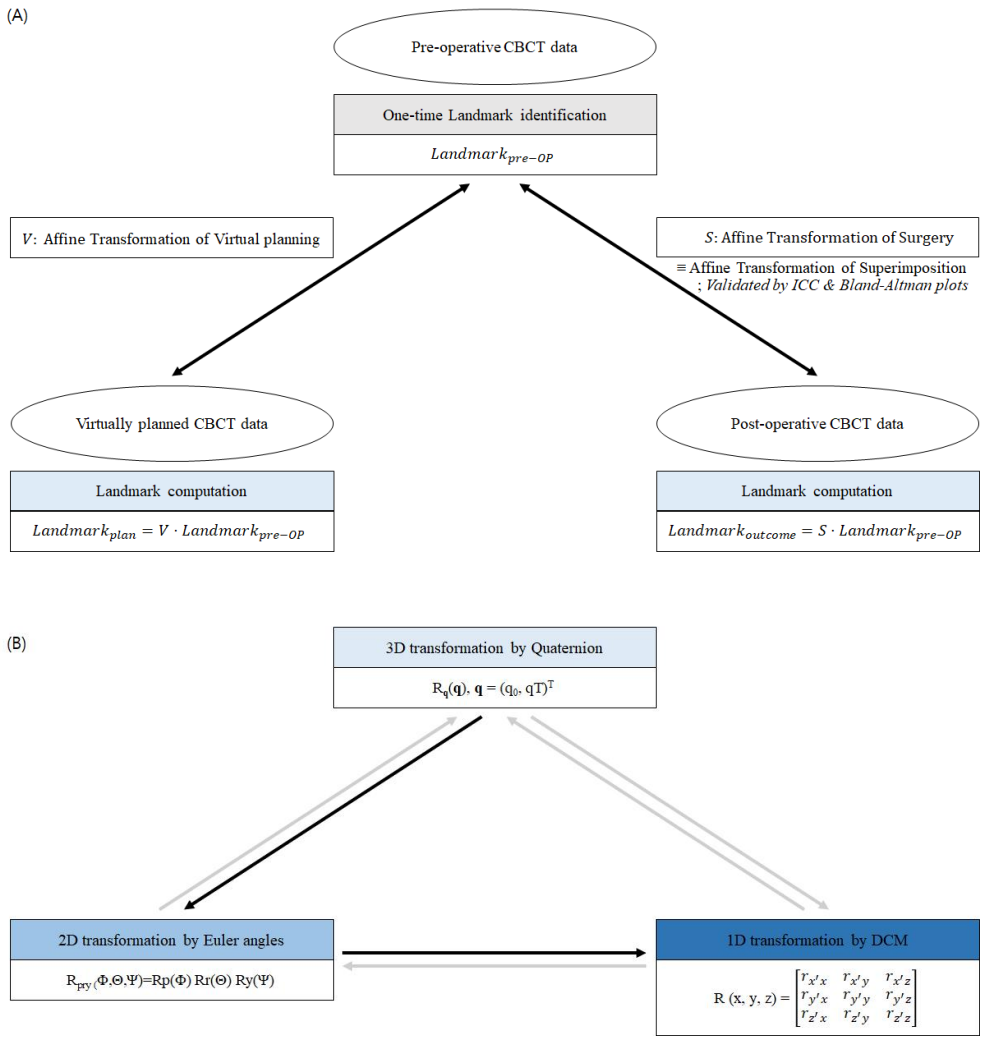

Figure 3 (A) The assessment process diagram. **(B)** Mathematical analysis using transformational relationships.

Abbreviations: CBCT, cone beam computerized tomography; ICC, Intraclass coefficient; DCM, Direction cosine matrix; $R_q(\mathbf{q})$, Rotation matrix by quaternion $\mathbf{q}$; q_0, scalar part of **q;** q, vector part of **q**; $R_{pry}(\Phi,\Theta,\Psi)$, Rotation matrix by Euler angles (pitch of Φ, roll of Θ, and yaw of Ψ); $R_p(\Phi)$, Rotation matrix by Euler angle (pitch of Φ); $R_r(\Theta)$, Rotation matrix by Euler angle (roll of Θ); $R_y(\Psi)$, Rotation matrix by Euler angle (yaw of Ψ); R (x, y, z), Rotation matrix represented by Cartesian coordinate, from $(x, y, z)^T$ to $(x', y', z')^T$; r, element of R (x, y, z).

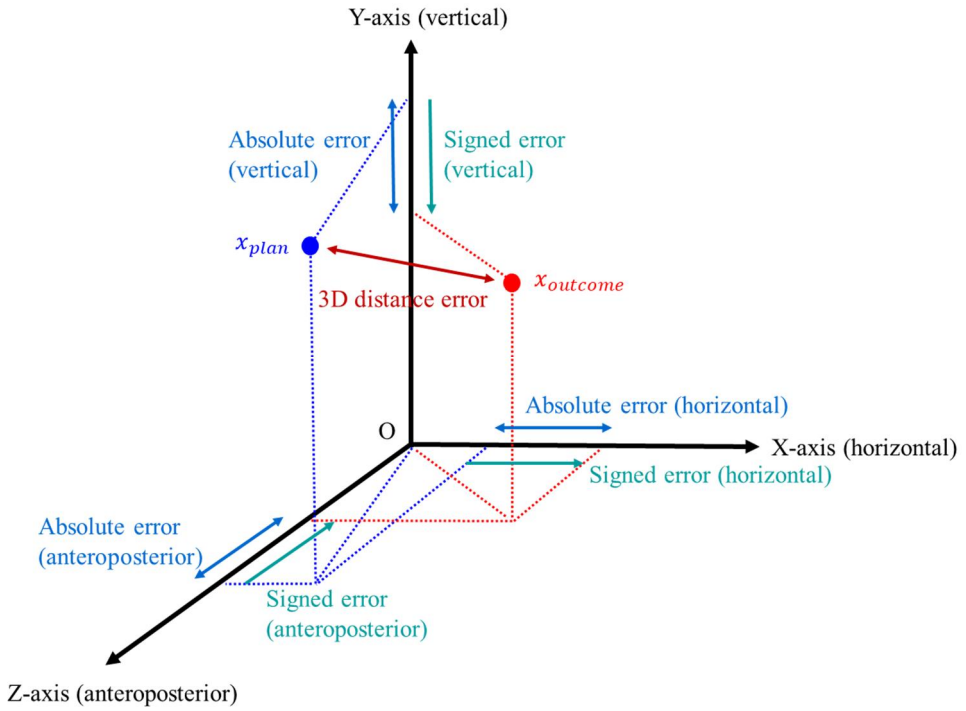

Figure 4. Three kinds of errors to evaluate surgical accuracy: mean three-dimensional (3D) distance error, mean absolute errors, and mean singed errors.

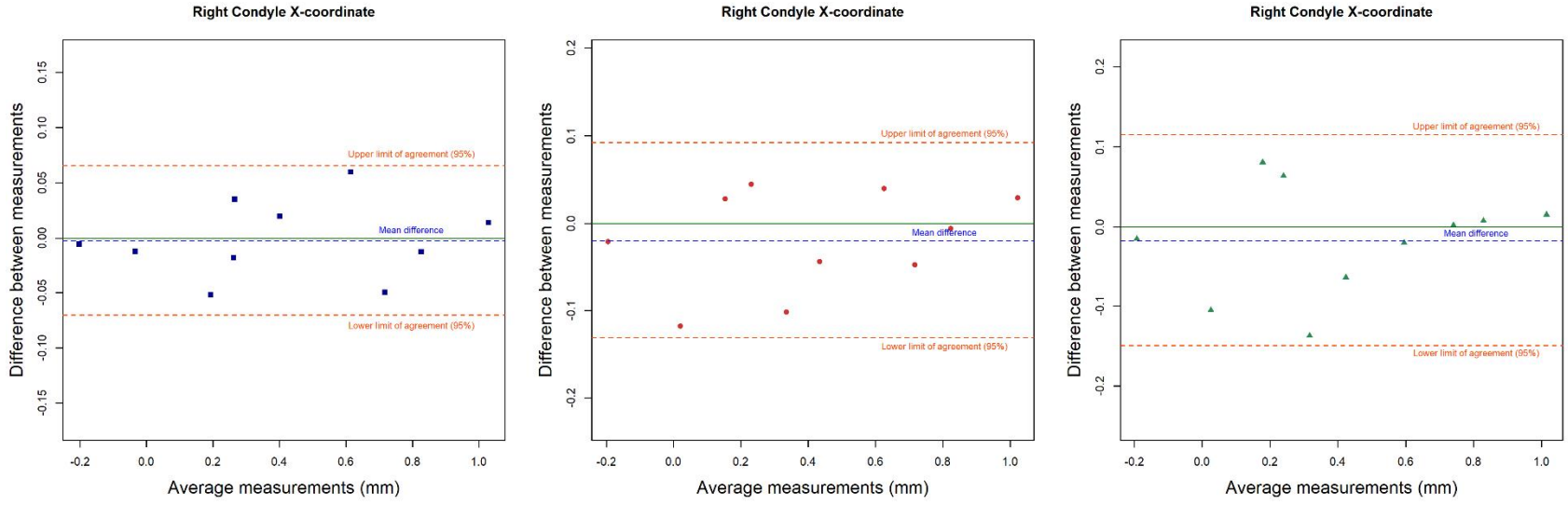

Figure 5. (A) Representative Bland–Altman plots for the right condyle: Agreement for X-coordinate.

Left, the agreement between two superimpositions of one researcher; Middle, the agreement between the first superimposition of one researcher and the superimposition of the other researcher; Right, the agreement between the second superimposition of one researcher and the superimposition of the other researcher.

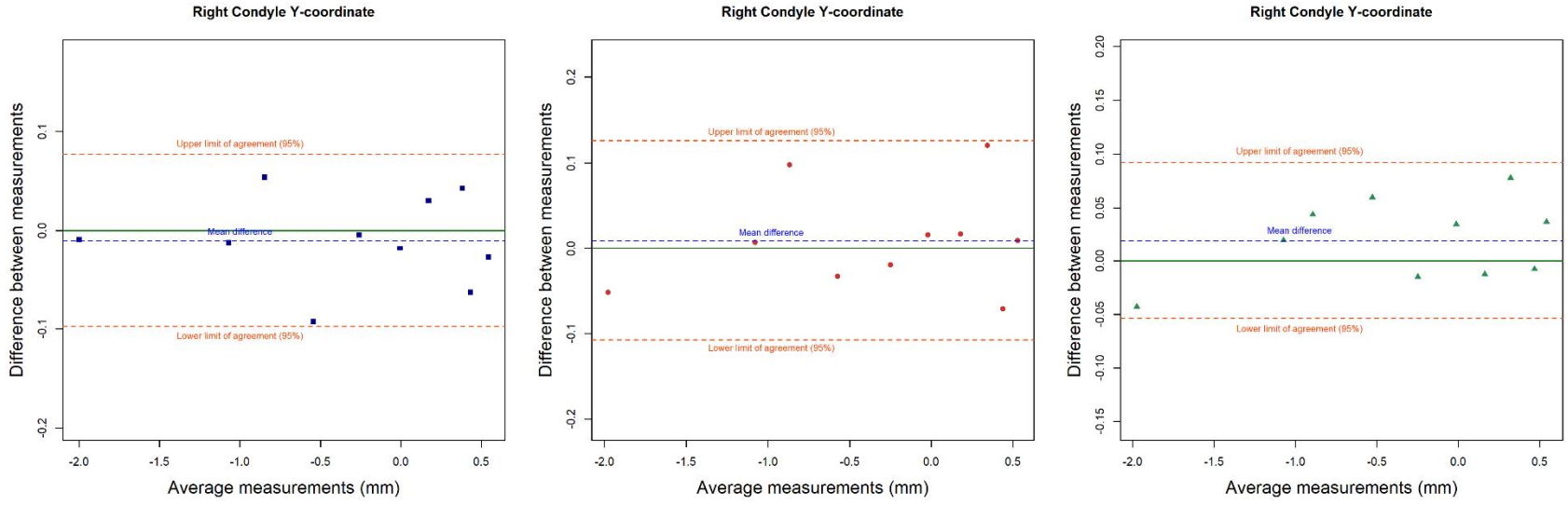

Figure 5. (B) Representative Bland–Altman plots for the right condyle: Agreement for Y-coordinate.

Left, the agreement between two superimpositions of one researcher; Middle, the agreement between the first superimposition of one researcher and the superimposition of the other researcher; Right, the agreement between the second superimposition of one researcher and the superimposition of the other researcher.

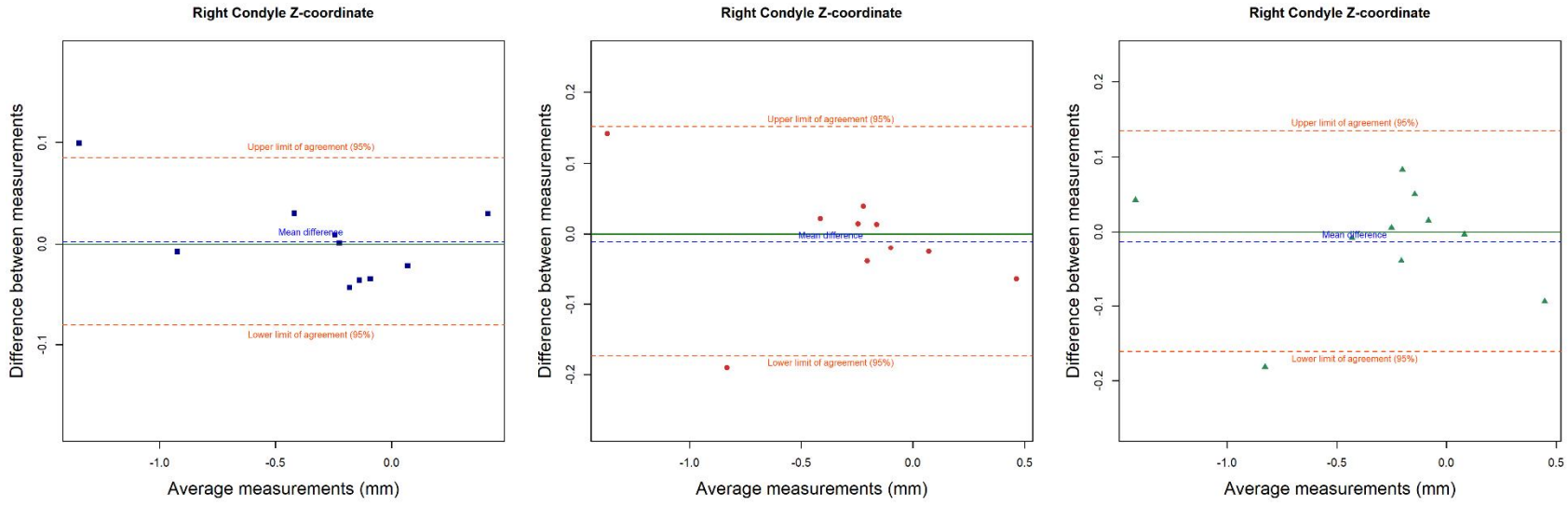

Figure 5. (C) Representative Bland–Altman plots for the right condyle: Agreement for Z-coordinate.

Left, the agreement between two superimpositions of one researcher; Middle, the agreement between the first superimposition of one researcher and the superimposition of the other researcher; Right, the agreement between the second superimposition of one researcher and the superimposition of the other researcher.

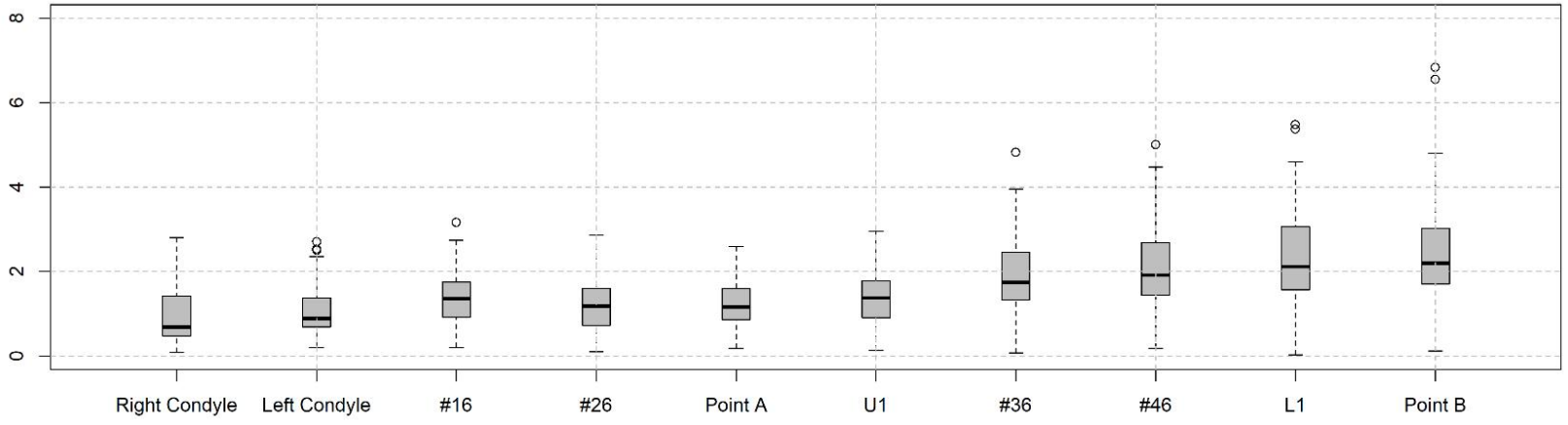

Figure 6. Box-and-whisker plot of the mean three-dimensional distance errors in three-dimensional space.

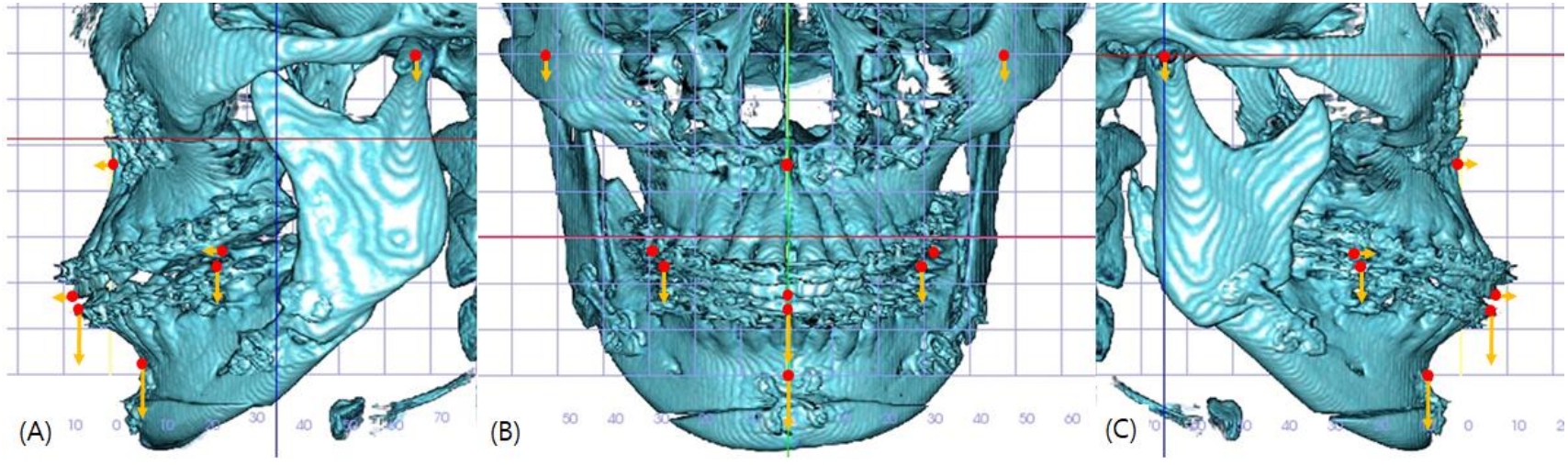

Figure 7. Magnitude and direction for mean signed errors of 10 landmarks. **(A)** Left side. **(B)** Frontal side. **(C)** Right side.

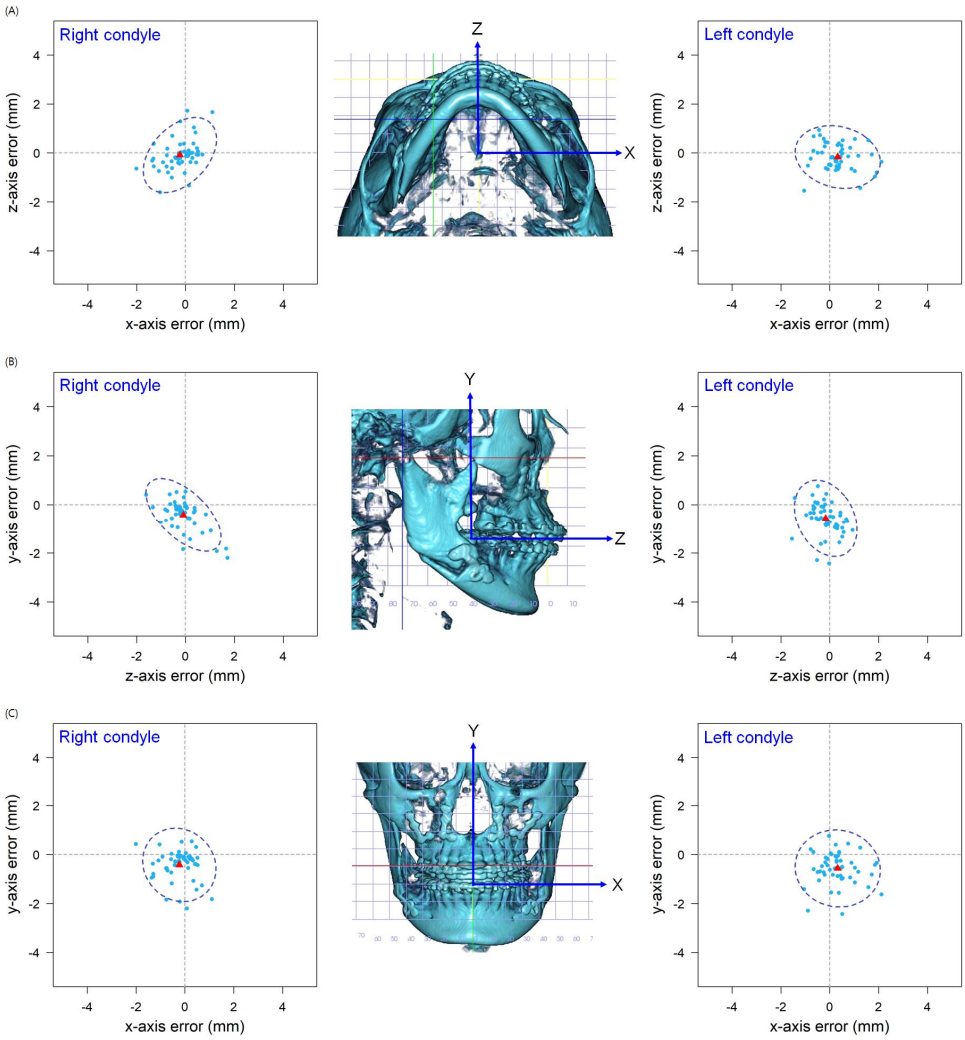

Figure 8. Scattergrams and 95% confidence boundaries for the errors of the right and left condyles. **(A)** Errors in the XZ plane. **(B)** Errors in the ZY plane. **(C)** Errors in the XY plane.

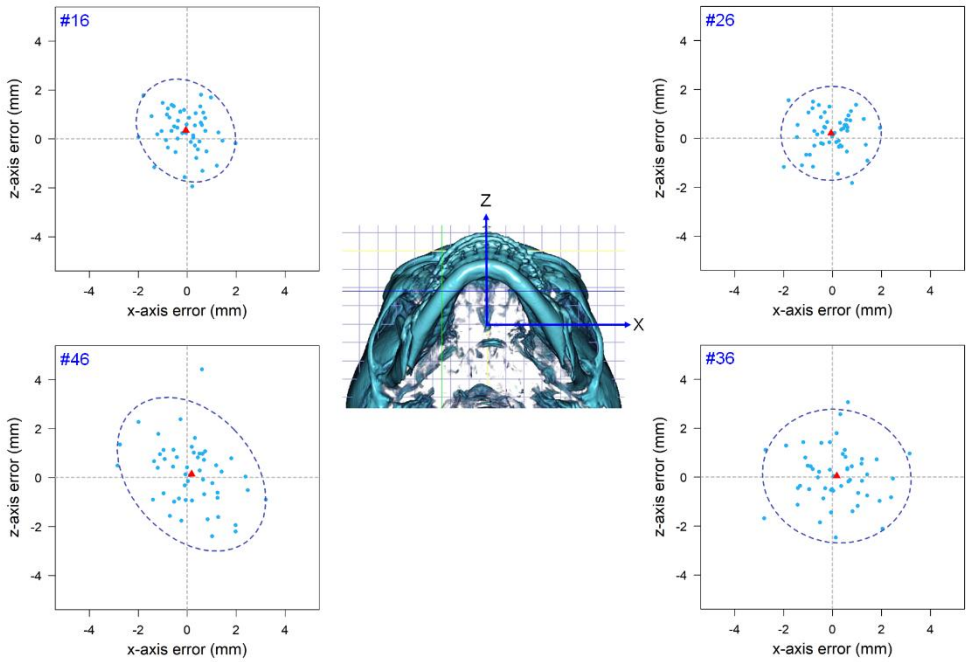

Figure 9. (A) Scattergrams and 95% confidence boundaries for the errors of maxillary right and left first molars and mandibular right and left first molars: Errors in the XZ plane.

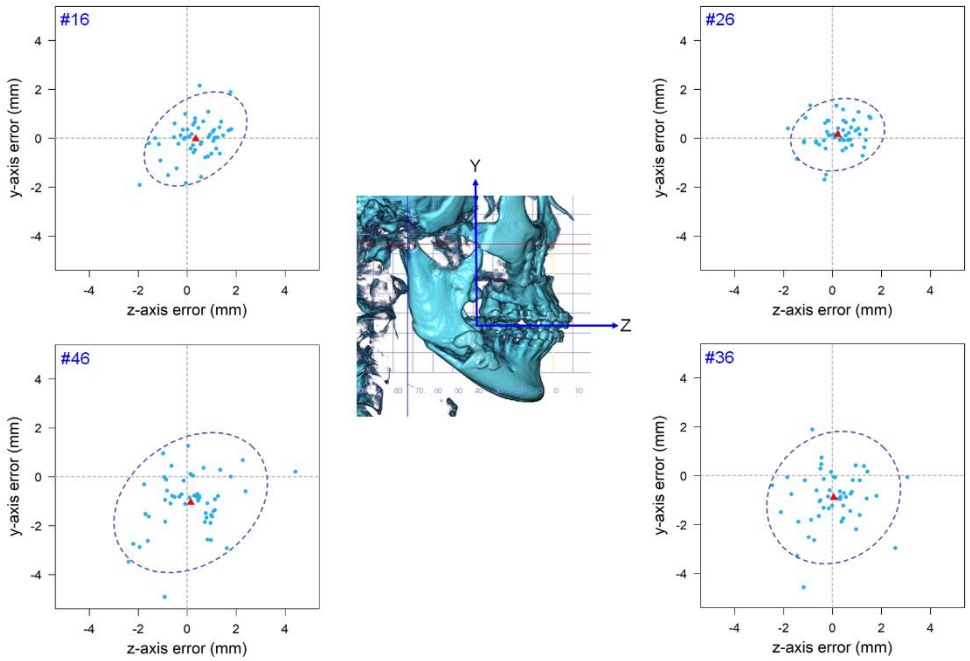

Figure 9. (B) Scattergrams and 95% confidence boundaries for the errors of maxillary right and left first molars and mandibular right and left first molars: Errors in the ZY plane.

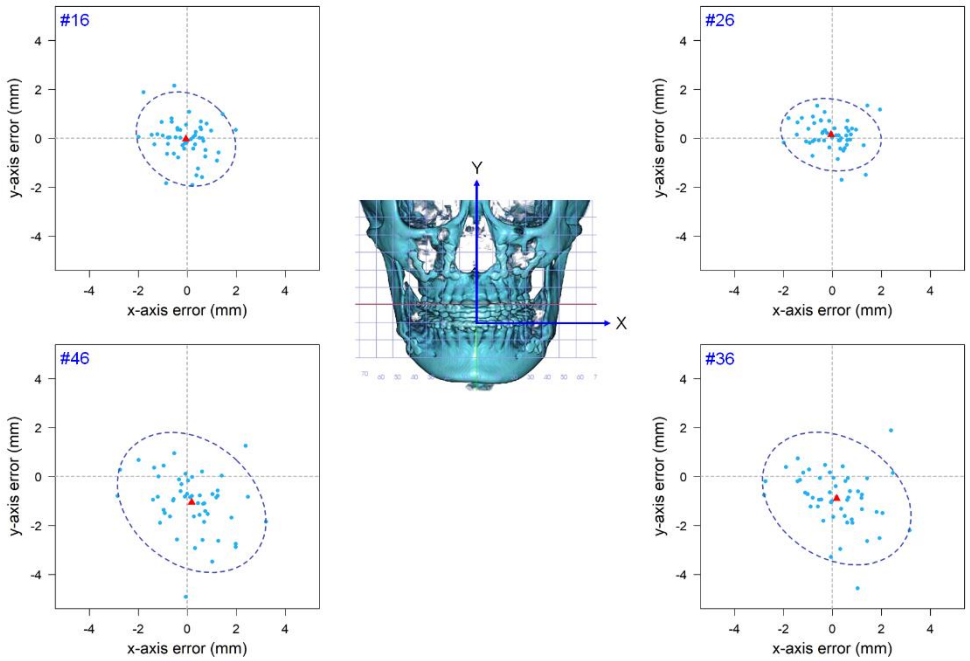

Figure 9. (C) Scattergrams and 95% confidence boundaries for the errors of maxillary right and left first molars and mandibular right and left first molars**:** Errors in the XY plane.

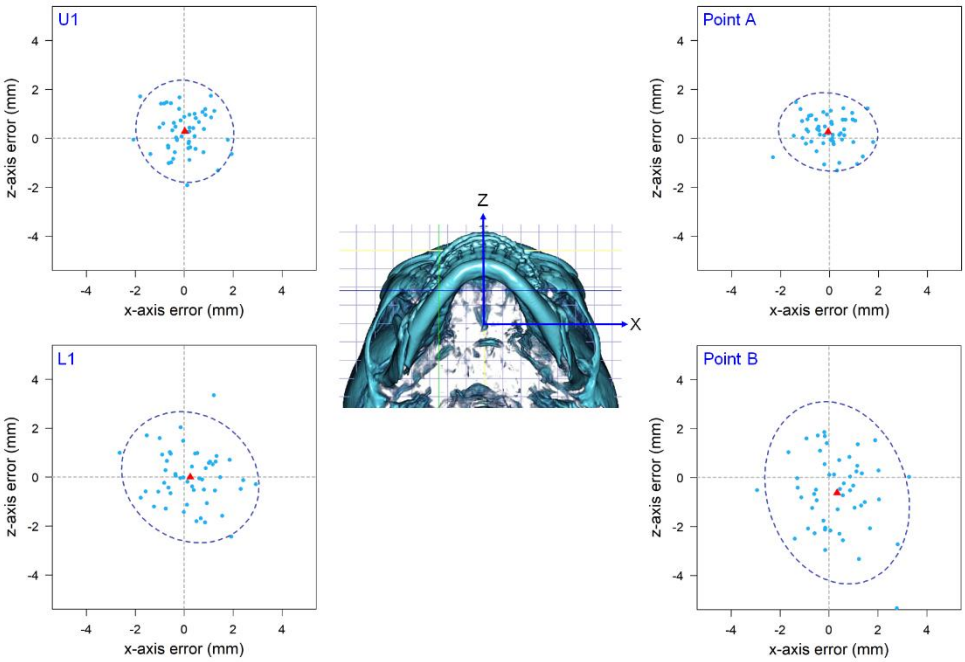

Figure 10. (A) Scattergrams and 95% confidence boundaries for the errors of U1, L1, Point A, and Point B: Errors in the XZ plane.

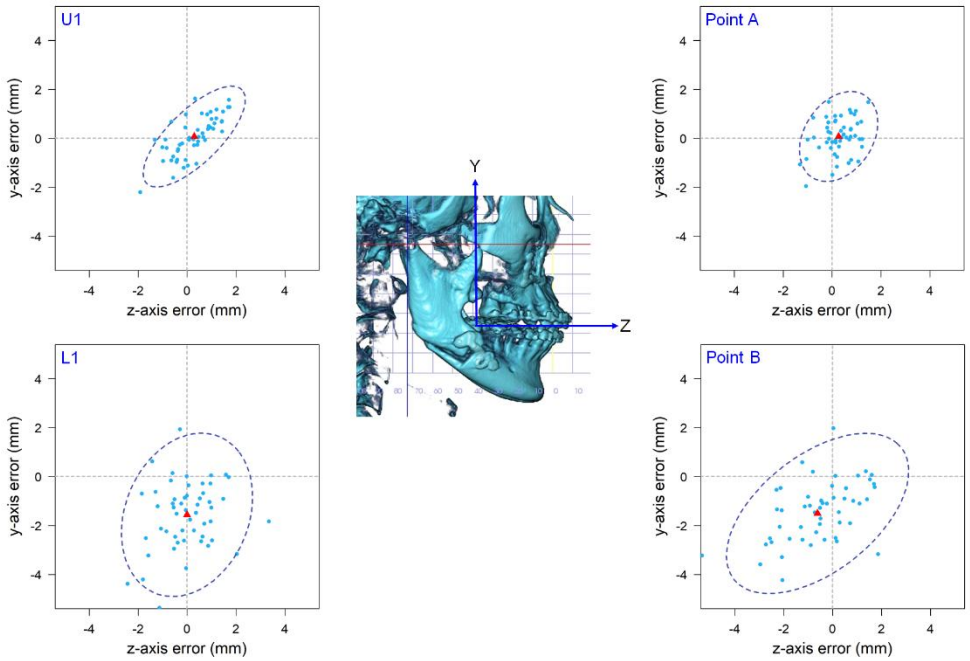

Figure 10. (B) Scattergrams and 95% confidence boundaries for the errors of U1, L1, Point A, and Point B: Errors in the ZY plane.

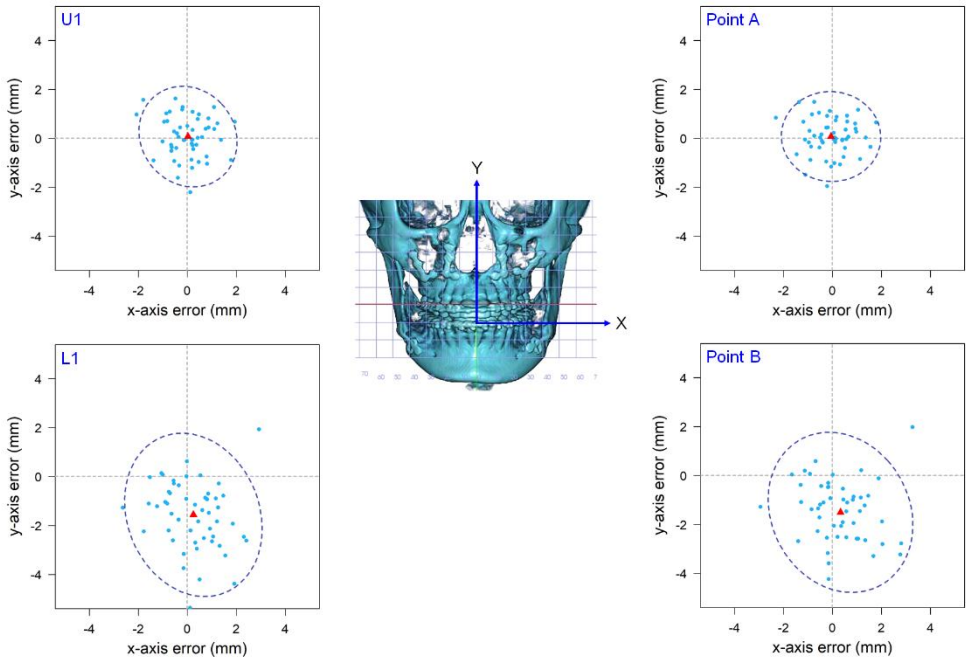

Figure 10. (C) Scattergrams and 95% confidence boundaries for the errors of U1, L1, Point A, and Point B: Errors in the XY plane.

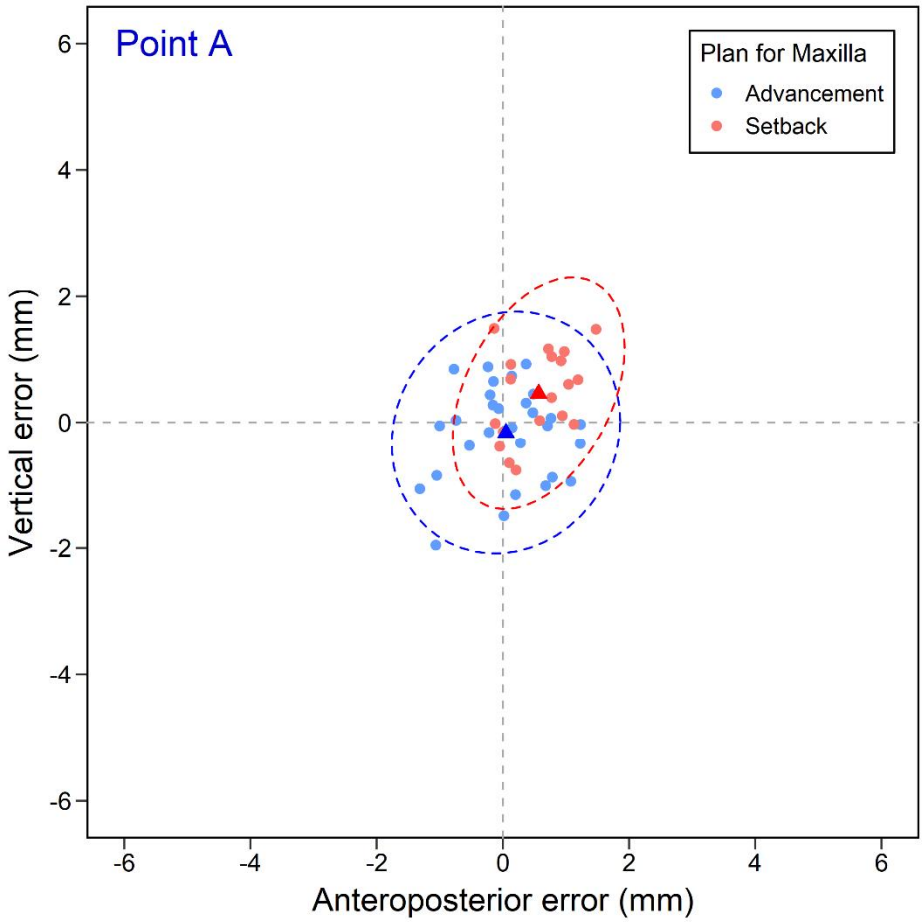

Figure 11. (A) Scattergram and 95% confidence boundary for the errors of Point A according to anteroposterior plan for the maxilla. The errors were illustrated for 48 subjects whose vertical plan for the maxilla was impaction.

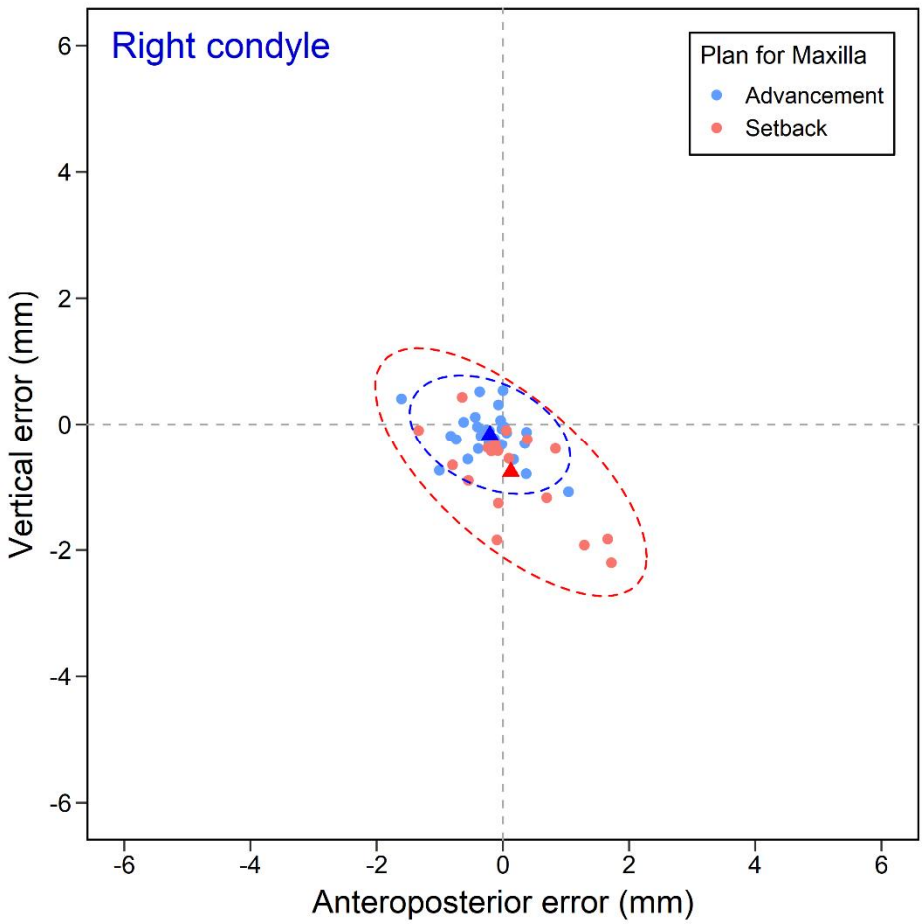

Figure 11. (B) Scattergram and 95% confidence boundary for the errors of the right condyle according to anteroposterior plan for the maxilla. The errors were illustrated for 48 subjects whose vertical plan for the maxilla was impaction.

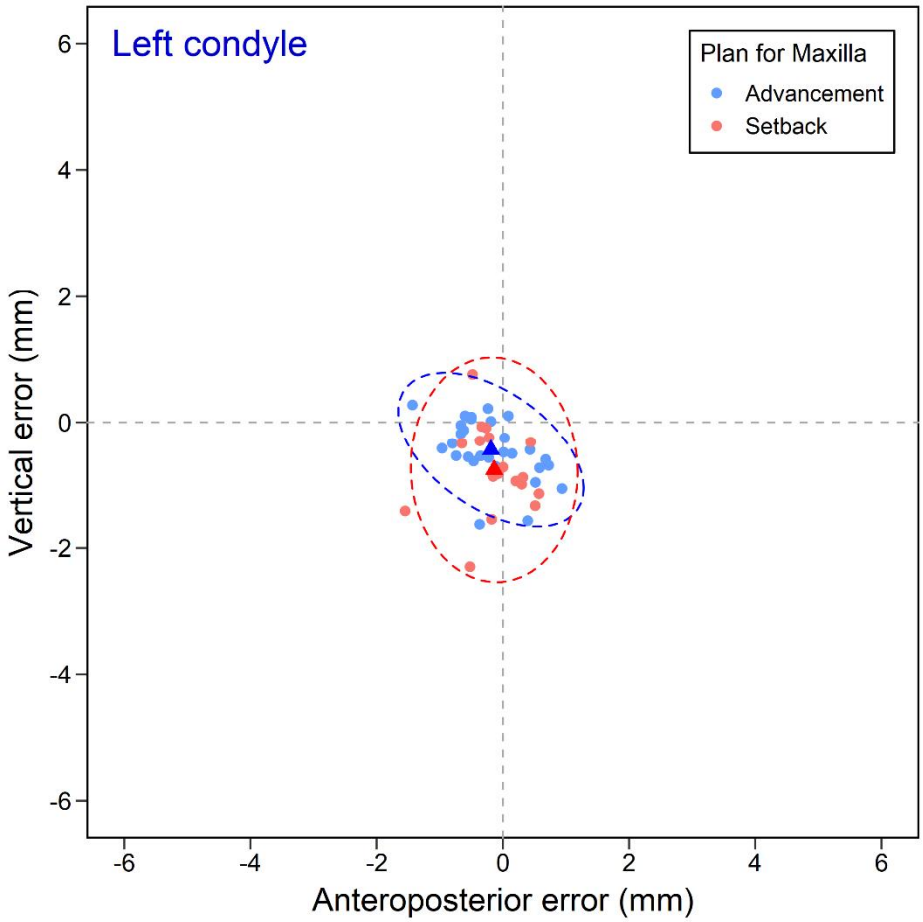

Figure 11. (C) Scattergram and 95% confidence boundary for the errors of the left condyle according to anteroposterior plan for the maxilla. The errors were illustrated for 48 subjects whose vertical plan for the maxilla was impaction.

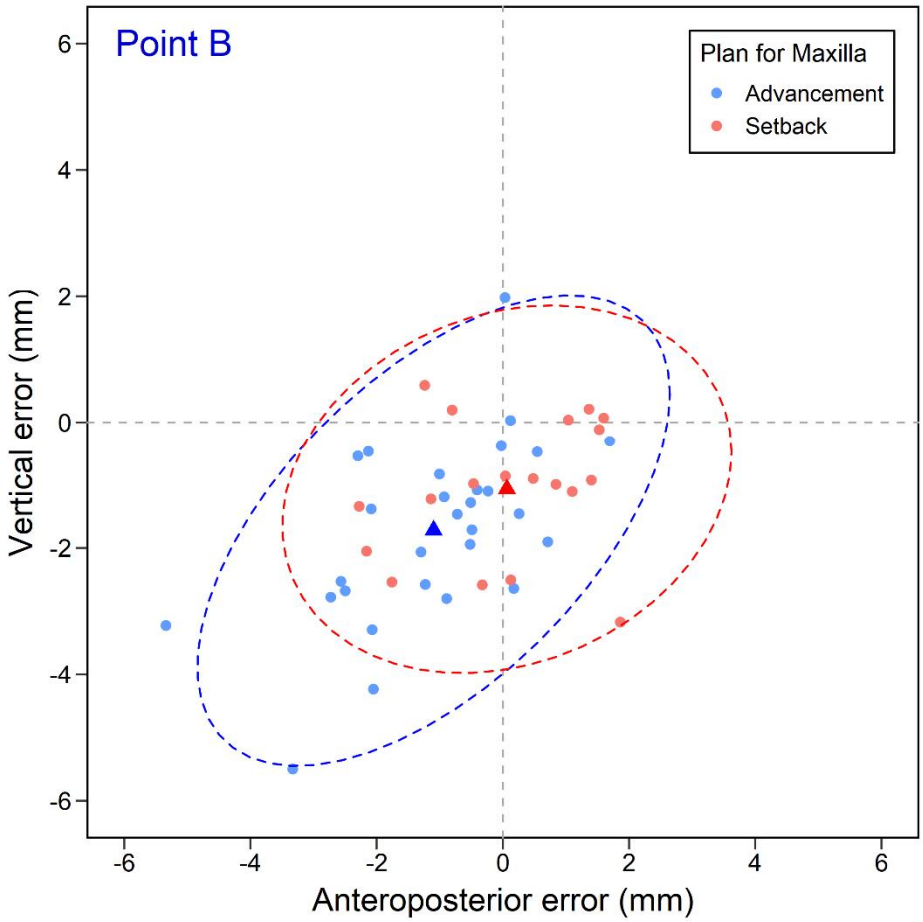

Figure 11. (D) Scattergram and 95% confidence boundary for the errors of Point B condyle according to anteroposterior plan for the maxilla. The errors were illustrated for 48 subjects whose vertical plan for the maxilla was impaction.

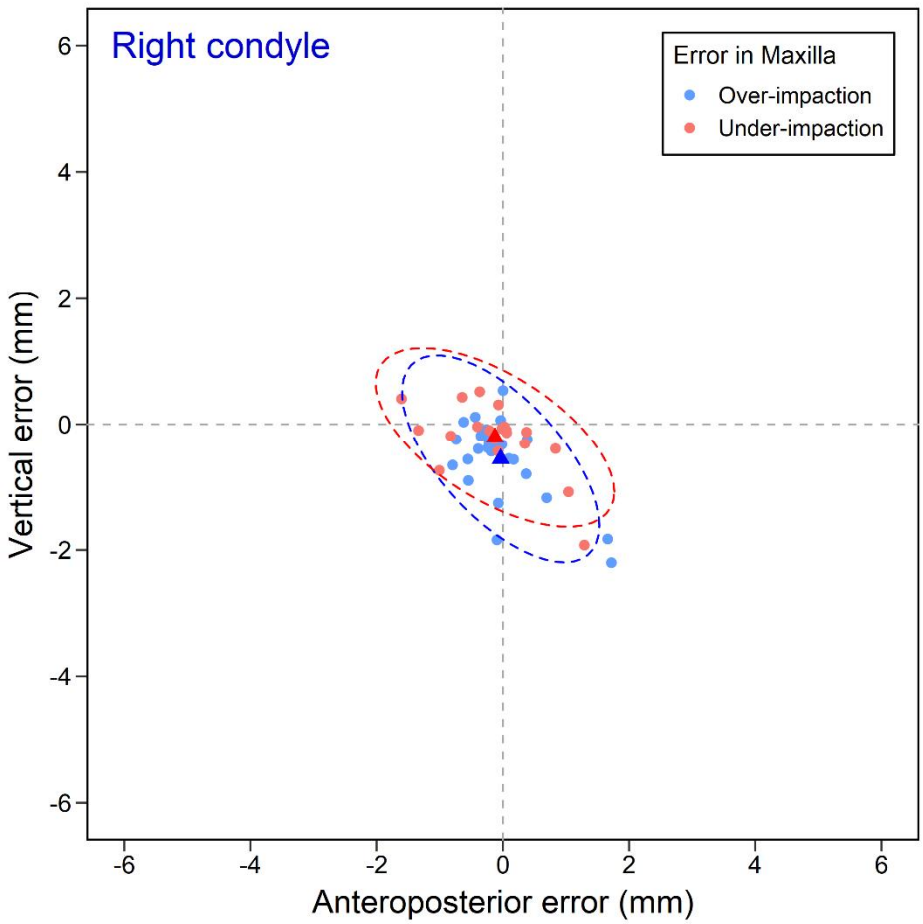

Figure 12. (A) Scattergram and 95% confidence boundary for the errors of the right condyle according to vertical error in the maxilla. The errors were illustrated for 48 subjects whose vertical plan for the maxilla was impaction. Over-impaction was defined as a case in which the amount of the maxillary impaction was larger than the planned. Under-impaction was defined as a case in which the amount of the maxillary impaction was smaller than the planned.

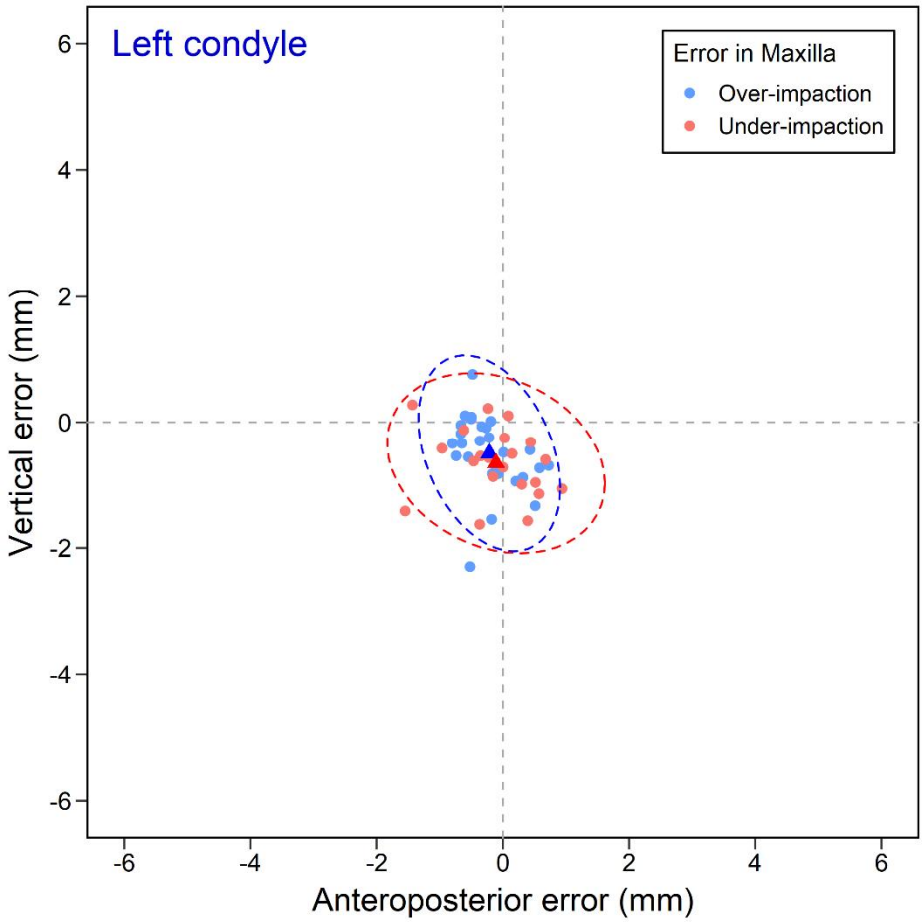

Figure 12. (B) Scattergram and 95% confidence boundary for the errors of the left condyle according to vertical error in the maxilla. The errors were illustrated for 48 subjects whose vertical plan for the maxilla was impaction. Over-impaction was defined as a case in which the amount of the maxillary impaction was larger than the planned. Under-impaction was defined as a case in which the amount of the maxillary impaction was smaller than the planned.

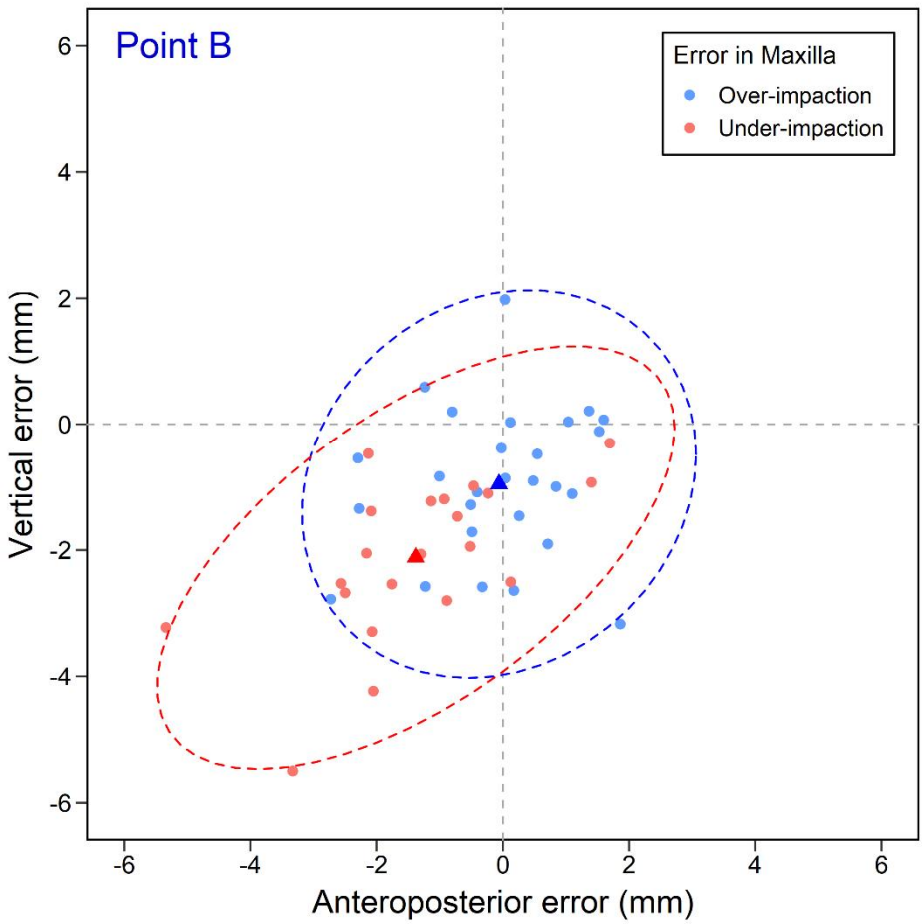

Figure 12. (C) Scattergram and 95% confidence boundary for the errors of Point B according to vertical error in the maxilla. The errors were illustrated for 48 subjects whose vertical plan for the maxilla was impaction. Over-impaction was defined as a case in which the amount of the maxillary impaction was larger than the planned. Under-impaction was defined as a case in which the amount of the maxillary impaction was smaller than the planned.

국문 초록

가상수술계획을 이용한

턱교정 수술의 정확도에 대한 연구

오 현 준

서울대학교 대학원 치의과학과 구강악안면외과학전공

(지도교수: **서 병 무**)

연구 목적: 최근 3차원 가상수술계획을 이용하여 턱교정 수술을 시행한 결과로서 수술 정확도에 대한 연구들이 보고되고 있다. 하지만 수술 정확도를 평가하기 위한 표준화된 방법이 없는 실정이며, 하악 과두를 포함하여 해부학적 위치별로 정확도를 분석한 연구는 거의 이루어지지 않았다. 본 연구의 목적은 계측점을 한번만 설정하면 되는 수학적 방법을 검증하고, 가상 계획과 수술 결과 간 오차의 정도와 분포를 각 해부학적 위치에 따라 분석함으로써 임상적 의미를 도출하는 것이다.

연구 방법: 본 연구는 한 명의 술자에 의해 상악과 하악을 함께 수술 받은 골격성 III 급 부정교합 환자들을 대상으로 하였다. 본 연구에서 사용한 가상수술계획은 콘빔 전산화 단층촬영 (cone beam computed

tomography)과 치아 모델 스캔을 기반으로 하였다. 악안면 급속 조형 (rapid prototyping) 모델과 수술용 스플린트 (splint)를 3차원 프린팅을 이용하여 제작하였다. 급속 조형 모델 상에서 골절단을 위한 수술용 가이드를 제작하고 금속판을 미리 구부려 사용하였다. 수술 결과를 평가하기 위해 술후 콘빔 전산화 단층촬영을 시행하였다. 하악 우측 과두, 하악 좌측 과두, 상악 및 하악 원심 골편의 네 가지 해부학적 위치들을 10개의 계측점을 이용하여 분석하였다. 각 계측점은 어파인 (affine) 변환에 기반한 수학적 방법을 이용하여 일회 계측점 설정 방식으로 측정하였다. 이 수학적 방법으로 계측한 측정치 간의 일치도를 평가하였다. 수술 정확도는 가상 계획과 수술 결과의 차이로 정의하였다. 정확도는 1) 3차원 데카르트 공간에서 평균 3차원 거리 오차, 2) 수평축, 수직축 및 전후축 평균 절대 오차, 3) 수평축, 수직축 및 전후축 평균 부호 오차의 3가지로 분석하였다. 다차원 산점도를 이용하여 평균 부호 오차를 도시하였다. 해부학적 위치와 수술 정확도 간 연관성을 측정하기 위해 이변량 분석과 회귀 분석을 시행하였다. 수술 정확도에 영향을 미치는 요인을 규명하기 위해, 상악의 수술 계획에 따른 정확도와 상악의 오차에 따른 정확도를 분석하였다.

결과: 본 연구는 남성 26명, 여성 26의 총 52명의 환자를 대상으로 하였고, 평균 나이 21세 3개월이었다. 일회 계측점 설정을 위한 수학적 방법은 측정치 간 뛰어난 일치도를 보였다. 하악 우측 과두, 하악 좌측 과두, 상악 및 하악 원심 골편의 평균 3차원 거리 오차는 각각 0.95, 1.12,

1.25 및 2.24 mm 였다. 세 좌표축 중 최대 오차를 보인 좌표축의 평균 절대 오차는, 하악 우측 과두, 하악 좌측 과두 및 하악 원심 골편은 모두 수직 성분으로 각각 0.51, 0.66 및 1.40 mm 였고, 상악은 전후방 성분으로 0.68 mm 였다. 세 좌표축 중 최대 오차를 보인 좌표축의 평균 부호 오차는, 하악 우측 과두, 하악 좌측 과두 및 하악 원심 골편은 모두 계획한 위치보다 하방 성분으로 각각 0.42, 0.57 및 1.25 mm 였고, 상악은 계획한 위치보다 전방 성분으로 0.28 mm 였다. 하악 원심 골편의 오차 분포가 과두와 상악보다 더 넓은 분포를 보였다. 상악과 과두의 오차는 상악을 전진시킬 때 보다 후퇴시킬 때 오차가 더 증가하였다. 하악 원심 골편의 오차는 상악의 상방 이동량이 계획량보다 작은 경우 더 증가하였다.

결론: 턱교정 수술의 정확도 분석에 본 연구의 계측점 설정 방법을 신뢰성 있게 사용할 수 있다. 가상수술계획을 이용한 턱교정 수술의 정확도는 해부학적 위치 중 하악 우측 과두와 좌측 과두가 가장 정확했고, 이어서 상악, 그리고 하악 원심 골편 순으로 정확했다. 수술 정확도는 상악의 수술 계획과 상악의 오차에 영향을 받았다. 정확한 턱교정 수술을 위해서는 각 해부학적 위치에서 수술 오차의 경향성을 고려하는 것이 중요하다.

주요어: 수술 정확도, 턱교정 수술, 가상수술계획, 골격성 III급 부정교합, 어파인(affine) 변환

학 번: 2017-32052

감사의 글

박사학위 과정을 진행하면서 많은 도움을 주신 여러 스승님과 동료, 가족에게 감사의 말씀을 올립니다.

연구와 임상, 그리고 진료하는 마음가짐에 이르기까지 소중한 가르침을 주신 서병무 지도교수님께 깊은 감사를 드립니다. 논문 심사위원장을 맡아주시고 귀중한 가르침 주신 최진영 교수님과 통계 작업에 큰 도움 주시고 귀한 가르침 주신 치과교정과 이신재 교수님께도 진심으로 감사드립니다. 또한 논문을 꼼꼼히 살펴주시고 격려해주신 박주영 교수님과 여러 고견을 주신 고대안암병원 구강악안면외과 송인석 교수님께도 감사드립니다.

임상과 연구에 대해 큰 가르침 주신 구강악안면외과학교실의 이종호 교수님, 명훈 교수님, 김성민 교수님, 양훈주 교수님, 서미현 교수님, 최원재 교수님, 한정준 교수님, 권익재 교수님께도 감사드립니다. 또한 의국 동기들과 선후배님들께도 감사드립니다. 그리고 통계 분석에 많은 도움을 주신 치과교정과 문준호 선생님께도 감사드립니다. 본 연구의 턱교정 수술 시 사용한 가상수술계획 시스템의 개발자 손홍범 원장님과 데이터 처리에 도움 주신 손인선 연구원님께도 감사의 말씀을 전합니다.

지금의 제가 있기까지 한결 같은 사랑과 정성으로 보살펴주시고 지원해주신 존경하는 아버님, 어머님께 깊은 감사를 드리며, 저를 늘 배려해주시는 장인어른, 장모님께도 진심으로 감사드립니다. 언제나 저를 응원해주신 외할머님과 동생에게도 감사드립니다. 저를 믿고 든든하게 내조해준, 인생의 동반자인 사랑하는 아내와 우리 보물 연우에게 큰 고마움을 전합니다. 감사합니다.

2021년 8월

오 현 준